NASA
Technical
Paper
2144

March 1983

A Study of Production of Miscibility Gap Alloys With Controlled Structures

R. A. Parr,
M. H. Johnston,
J. A. Burka,
J. H. Davis,
and J. A. Lee

NASA

NASA
Technical
Paper
2144

1983

A Study of Production of Miscibility Gap Alloys With Controlled Structures

R. A. Parr,
M. H. Johnston,
J. A. Burka,
J. H. Davis,
and J. A. Lee
George C. Marshall Space Flight Center
Marshall Space Flight Center, Alabama

National Aeronautics
and Space Administration

**Scientific and Technical
Information Branch**

TABLE OF CONTENTS

LIST OF ILLUSTRATIONS

LIST OF ILLUSTRATIONS (Concluded)

LIST OF TABLES

TECHNICAL PAPER

A STUDY OF PRODUCTION OF MISCIBILITY GAP ALLOYS WITH CONTROLLED STRUCTURES

INTRODUCTION

Miscibility gap alloy systems have largely been neglected in past years because of processing difficulties which usually produce an inhomogeneous solid state structure. More than 500 alloy systems have been identified in which there is immiscibility to some extent in the liquid state [1]. As a class these alloys have remained unexplored, and they represent a sizable gap in our knowledge and understanding of the physics of solids. It has been projected, based on their elemental content, that many immiscible combinations, if available as homogeneous alloys, would exhibit desirable physical properties. Superconductors, bearing materials, composites, and enhanced thermal conductors are several of the desirable properties that might be obtained by successful processing of miscibility gap materials.

One of the miscibility gap alloys studied was the aluminum-bismuth system, and its associated phase diagram is shown in Figure 1 [2]. Within the miscibility gap there are two liquids in equilibrium that transform below the monotectic temperature into aluminum and bismuth. Thus, the solubility of bismuth in aluminum at room temperature is negligible. Another inherent problem with these alloys is the sedimentation effect resulting from liquids having different densities and gross density differences between the resultant solid components. The densities of aluminum and bismuth are 2.70 g/cc and 9.80 g/cc, respectively. The other property that causes difficulty in processing miscibility gap materials is their wide variation of melting points between components. The melting point of aluminum is 660°C while bismuth is 271.3°C; thus, separation of the pure elements during solidification results in bismuth remaining molten within the solid aluminum.

The most obvious means of controlling the final solidification product of miscibility gap materials is processing in a low-gravity environment whereby sedimentation is substantially reduced. One such proposal by the authors was selected by NASA Headquarters for Spacelab Category III ground base testing. Extensive studies were performed on several candidate miscibility gap materials. During the course of this investigation a processing technique was discovered and subsequently became a NASA patent [3]. An aluminum-bismuth alloy was modified with a dopant material and directionally solidified under cellular growth conditions to produce a uniform dispersion of bismuth in aluminum (Fig. 2) [4,5]. This new process required high thermal gradients and a small diameter sample (2 mm) to effectively control the convection and thermal gradients in the sample. Two MSFC Discretionary Fund Projects were obtained to further study the process parameters. These provided for baseline studies of D.S. production of alloys that may provide a significant advantage over prior processes.

One of the alloys selected for study was Cu-Nb, a system that would have commercial feasibility as a superconductor. The phase diagram for Cu-Nb is given in Figure 1. The goal of superconductor fabrication is generally to produce a very long length of wire in the form of a metal-matrix composite consisting of a very large number (approximately 1000) of fine filaments (diameters between 5 and 60 μm) imbedded in a high-conductivity matrix of OFHC copper (but occasionally of aluminum).

Early magnets, which used single filaments of copper coated wire, rarely reached their design capability due to magnetic instabilities and flux jumps. It was later shown [6] that if the filament size was reduced, the movement of the flux lines were inhibited and the material was stable. In order to maintain

the capability to carry a large amount of current, but also remain stable, composites of many fine filaments were needed in a stabilizing matrix. The conventional way of doing this is to assemble the required number of copper-clad superconductor rods, plus copper filled pieces, into a copper can fitted with nose-cone and tail plug and suitably evacuated in readiness for extrusion. The "conventionally" or hydrostatically-extruded product is cold drawn to rod on a drawbench and further cold drawn to wire using a bullblock and a multidie machine in succession. The output of this process is a multifilamentary strand which, after insulation, can either be used in that form for the winding of small solenoidal magnets, or can be assembled with many others of its kind into a cable in order to enable the transportation of heavy supercurrents in large-scale applications.

Recently, experimenters have attempted to simplify the production by going to "in situ" superconducting wire. In this process either chill casting or consumable arc melting are used to produce a dendritic copper matrix. The niobium is uniformly dispersed throughout the casting. The ingot is then mechanically reduced to wire form, this procedure serving to elongate the niobium and to force the particles into continuity. Tin is later diffused into the wire to produce Nb_3Sn. Some standard casting problems still remain however. The ingot can contain porosity or areas of macrosegregation and impurities.

The purpose of this study was to determine the effectiveness of the MSFC directional solidification process for producing aligned niobium in a copper matrix by a one-step process.

EXPERIMENTAL PROCEDURE

A directional solidification system was used to produce a broad range of temperature gradients and growth rates. The system consists of a high temperature furnace with integral water-cooled quench block (Fig. 3). The 2 mm diameter sample remains stationary while the furnace with the quench block moves by a threaded rod and gear system. Using a test sample, the growth rate was determined to be equal to the rate of furnace movement. Temperature gradients were measured using dummy cartridges.

The Al-Bi-Fe samples were prepared by melting pure (99.999 percent) materials together in air at a temperature 200°C above the liquidus. The melt was cast and drawn into the required 2 mm diameter wire.

These were then solidified at rates of 0.5 to 21 cm/hr with temperature gradients of 150° to 410°C/cm and temperature gradient (G) to growth rate (R) values from 0.7×10^5 to 2.3×10^6°C/sec/cm^2 Figure 2 shows typical aligned rod and sphere structures in the Al-Bi-Fe system.

The Cu-Nb samples were prepared by weighing the appropriate amounts of 99.999 percent copper and niobium and melting them in argon between 1600°C and 1700°C. When required, the dopant 0.25wt%Al) was added at this stage. The resultant slug was then rolled into the desired wire size for processing. After processing, the samples were removed from the crucibles, then mounted and polished longitudinally. The minor constituent was clearly visible. Areas for cross sectioning were selected and polished.

The Cu-Nb system was found to solidify with an aligned structure when 0.25% aluminum was added as a dopant. Figure 4 shows typical examples of the processed structure.

When the morphology was well characterized, intact samples 30 mm to 60 mm long were analyzed for their superconducting properties by the University of Alabama, Huntsville. A total of 12 specimens were tested. The list of the specimens and their compositions is shown in Table 1. The detailed fabrication

processes used for preparing the samples for superconductivity measurements are given in Table 2. The first six specimens were prepared by Materials and Processes Laboratory, MSFC. The samples containing tin, 81CNA47-S and 81CNA7-B, were prepared by hot dipping into molten tin and diffusing it at temperatures up to 650°C, in an attempt to form the compound Nb_3Sn, which has a critical temperature (Tc) of 18°K. However, no significant effort was made to optimize the diffusion and reaction parameters for forming the compound. The last six specimens [8] were received from Dr. E. W. Collins, from Battelle Columbus Laboratory in Ohio. Figure 5 shows a typical structure as received from Battelle. Figure 6 shows the structure after directional solidification in Materials and Processes Laboratory.

Each specimen from Table 1 was tested by plotting the following curve:

1) The graph of the residual resistivity as a function of the specimen current density at 4.3 K.

2) The graph of the electrical resistivity as a function of the temperature at a constant current density.

The four probe technique of electrical resistivity measurement was used to ascertain if the specimen was superconducting. A specimen holder and its components are shown in Figure 7. The specimen holder is a small piece of IC board (4 x 2.5 cm). On this board are four elastic, gold-coated probes which secure the regular sized specimens. Thin specimens are secured by solder. The two outer probes pass a known current through the specimen by 22 gauge Soldereaze magnet wires. The voltage developed across the inner probes is then measured by 28 gauge Soldereaze magnet wires connected to a Keithly 148 nanovoltmeter.

The distance between the inner probes is approximately 1.6 cm. The voltage is proportional to the electrical resistance of the specimen. The resistivity is found by knowing the dimensions of the specimen. For reference purposes, the gross cross-sectional areas of the specimens are listed in Table 1.

In order to measure the temperature, a resistance thermometer is also attached to the specimen holder. There are two resistance thermometers being used; the Platinum-Resistance-Thermometer (PRT) and the Germanium-Resistance-Thermometer (GRT). The PRT is used when the temperature is between 60K to 300K, below 60K the GRT is used since the PRT loses its sensitivity to use at low temperature. In addition, a DPDT control switch is used to reverse the direction of the applied current DPDT through the specimens.

RESULTS

When the aluminum-bismuth samples were solidified with 0.2wt%Fe as a dopant, the bismuth aligned as either rods or spheres in the aluminum matrix. The theory behind the phenomena of the dopant was presented in the earlier paper [4]. The breakdown from rods into spheres must be concurrent with the solidification process since extensive heat treatment subsequent to processing, does not produce similar alignment. If spheres do finally form, they are irregularly spaced with varying sizes. The occurrence of the regular spacing of the spheres during solidification, is being discussed in another paper.

It was also necessary to add a dopant (0.25wt%Al) to the copper-niobium system in order to obtain alignment. The niobium adopted one of three morphologies during processing; aligned rods, rosettes, and cuboidal rods (Fig. 6).

Selected specimens were analyzed for distribution of the alloy elements by three instruments (electron microprobe at Georgia Tech, Kevex at the Space Science Laboratory, and EDAX at the Materials and Processes Laboratory of MSFC). Specimen 81CNA42, shown in Figure 8, was analyzed by microprobe in the representative areas indicated on the photomicrograph and results are given in Table 3. The aluminum has segregated mostly in the niobium rosettes with less than the nominal 0.25 percent of the copper matrix. The very low percent of niobium found in the small rods is contrary to their etching behavior and, as will be seen later in analyses by Kevex and EDAX, is believed to be caused by the probe beam being much larger than the rods and analyzing mostly the copper matrix.

Specimen 81CNA41 was analzyed by EDAX in the areas shown in Figure 9. This specimen was given a deeper etch than for 81CNA42 to reduce the matrix effects around the rods. Results of the analysis are given in Table 4.

The segregation of aluminum in the larger stringer agrees with results obtained with the microprobe on the rosettes, and the higher niobium content in the small rods shows the effect of deeper etching. The reason for not detecting aluminum in the small rods is not known.

The Kevex analyses of specimen 81CNA52 is shown in the spectra of Figure 10. The spectra of the fine rods agrees approximately with the EDAX analyses. (The presence of chromium in the spectra probably results from internal components of the SEM.) The coarse rods, of two types (right angle and rectangular) as shown in Figure 6, consist of nearly 100 percent niobium for the right angle type and predominantly niobium for the rectangular. No aluminum was detected in any of the spectra. Source of the silicon is not known.

Figure 11 shows the electrical resistivity as a function of temperature for the NASA specimens. According to the calibration specimen C-5 (99.5 percent pure copper), the resistivity varies form 0.65 to 0.72 micro ohm-cm when the temperature increases from 4.3K to 14K. The specimen which has the largest transition temperature range (ΔT) is 81NbBr53 (from 5.5K to 14.5K); while NbBr169 has the smallest transition temperature range, (the smaller the transition temperature range the higher the slope of the transition curve). Notice that at 4.3K, specimen 81CNA47-S does not give a zero-resistivity value, i.e., a magnitude of 0.5 micro ohm-cm is recorded. In addition, it has the highest normal resistivity value for the set.

The electrical resistivity versus temperature for the Battelle specimens is given in Figure 12. Specimen A-4 has the highest normal resistivity value when the sample is at 9.4K. All specimens shown in this figure have a temperature range from 7.3K to 9.7K.

Table 5 is a list of the resistivity-temperature characteristics of all 12 test specimens. It includes the specimen's current density using the normal resistivity, and the temperature range at which the transition of resistivity value takes place as a function of temperature. The resistivity-current characteristics for the twelve specimens are given in Table 6.

Figure 13 shows the current-voltage relations at 4.3K for sample C-5, 81NbBr53, 81CNA51, and 81CNA1700. Sample C-5 represents copper (99.5 percent pure) which has a linear current-voltage relation. This results in a constant value of resistivity as a function of specimen current shown in Figure 14. The resistivity value for copper fluctuates slightly around 70 nano ohm-cm, which is acceptable for reference purpose [7]. Above the C-5 curve is the current-voltage relation for specimen 81NbBr53. This specimen

produces a nonlinear I-V relation which has a sharp decreasing slope from 0.5 to 2.5 A current range. From 2.5 to 5.5 A, the I-V slope is constant; this results in a linear resistivity-current relation as shown in Figure 15, below 0.8 A. The R-I curve seems to exhibit some "negative resistivity" values in small magnitudes. Sample 81CNA51 has almost an identical I-V curve as of sample 81NbBr53, however; 81CNA51's curve has slightly higher value in resistance. The results in resistivity-current relation are shown in Figure 16; note that the sample tends to have small "negative resistivity" values when the sample current is below 0.25 A. Sample 81CNA1700 (Fig. 17) shows a very interesting current-voltage relation: from 0.5 to 7.5 A, the voltage increase is very small, but when the current is greater than 7.5 A, the voltage increases rapidly. The current-voltage relations for samples A-3, A-4, B-1, and NbBr 169 are shown in Figure 18. Note that for current ranges from 0 to 8.5 A, the specimens' voltage responses are small in magnitude (about 3.5 microvolt maximum). Samples A-3, A-4, and B-1 show very interesting I-V characteristics; i.e., when the positive current is applied the samples produced a small (pico-ohm-cm) negative voltage response. The phenomena also occurs for sample NbBr 169, and samples A-5 and B-4 (Fig. 19a,b,c). This results in the "negative resistivity"-current characteristics as shown in Figures 19b and 19c for A-5 and B-4, respectively. For sample A-5 the positive resistivity exists when the current is greater than 4.8 A. For sample B-4 the positive resistivity requires that current applied has to be greater than 2.6 A.

Figure 20 shows current-voltage relations for sample 81CNA47-B and 81CNA47-S. A small negative voltage response exists for 81CNA47-B, but this effect could be observed in detail by using the plot of resistivity versus current as shown in Figure 21. However, for sample 71CNA47-S (Fig. 22), "negative resistivity" did not exist even with a small positive applied current.

From the R-I relations, we may conclude that most of the tested specimens exhibit critical currents at 4.3K. Sample 81CNA1700 shows a sharply defined value of critical current, however, its normal resistivity value has not been recorded. Specimens A-3, A-4, and B-1 did not exhibit critical current at 4.3K. Their maximum applied current was 8.5 A. Higher currents are required so that these specimens would show their critical current at 4.3K. This means that the critical current densities for A-3, A-4, and B-1 should be very high, since these specimens have small cross-sectional areas. Specimen 81CNA47-S has a small but measurable resistivity at 4.3K, even with very small value of applied current. However, this specimen also has the normal resistivity characteristics when the applied current of 1 A is reached.

As mentioned earlier, when a positive current is applied to some of the specimens, it produced a negative voltage response. This negative effect has not been noticed in literature. This negative resistivity might be related to several possibilities; the superconductive tunnelling effect [9], or Josephson's tunnelling effect [10], or the normal electron tunnelling effect, since all tested specimens are composite superconductors, e.g., filaments of niobium wires are grown in copper matrices. (Tunnelling effects may result from a system of two superconductors with a thin insulator [11]). A less esoteric cause might be thermal emf., heating effect by the applied current, or reliability on the measurement recorded by the experiment apparatus.

The ohmic heating produced sample thermal profile is invariant [12] with respect to current direction and, thus, is readily subtracted on current reversal. On the other hand, this "negative resistance" is possible due to Peltier junction heating [10,13]. These resulting thermal gradients would also change direction upon current reversal and, thus, would become a non-subtractable-error (Seebeck voltage) in the bulk resistance. Although Peltier heating increases linearly with current, it is apparently overwhelmed by the greater rate at which the current drives the sample normal through the superconducting transition [equation (1)]. Typically, a pure element sample Peltier heating is only a few tenths of a microwatt, thus, generating a Seebeck voltage of only a few tenths of a nano-volt. However, upon alloying, the cryogenic Seebeck coefficients S_A easily increase by one or two orders of magnitude. The current density (I/A) would increase locally in the superconducting filament region. The alloying could decrease the thermal conductivity (K) by one or two orders of magnitude (neglecting the K of the He medium). In equation (1):

$$V = (S_B - S_A)^2 \frac{TIL}{KA} \tag{1}$$

Since the equation is quadratic in S, a six or seven order of magnitude increase in V (into the micro-volt range), although unlikely, is not impossible. T is the absolute temperature and L the sample length. S_A and S_B are the Seebeck coefficients of the sample and wires (Cu), respectively. The apparent resistivity, $\rho a(T)$, is given as the sum of the true resistivity, $\rho(T)$, and the error (Seebeck) term.

$$\rho_a(T) = \frac{VA}{IL} = \rho(T) + (S_B - S_A)^2 \, T/K \tag{2}$$

As T approaches T_c, $\rho(T)$ approaches zero and the Seebeck term eventually dominates.

The following improvements (all unsuccessful) were made to identify the "negative resistance" voltage source:

1) Enhancing the interelectrode isolation resistance from 10^4 ohms to about 100 Mohms by replacing the magnet wires (leads) with untwisted magnet wires.

2) Uncoiling the current wire coil near the sample to prevent magneto-resistance.

3) Installing a current reversing switch.

4) Calibrating the nanovoltmeter with a nanovolt source.

5) Increasing the sample depth under L. He to six inches.

6) Replacing the current supply with a wet cell (automobile) for better isolation.

7) Using two continuous synchronized strip chart recorders to monitor sample voltage and current.

Future researchers may wish to use a Faraday cage room, interchange nanovoltmeter, or use a SQUID voltmeter.

All in all we are 80 percent confident that the negative voltage is real. We are 30 percent confident that it is Seebeck related. Our confidence that it is Peltier related is only 10 percent, however.

CONCLUSIONS

1) A negative response to a certain positive range of current exists for nine of the twelve specimens tested. Battelle's specimens show a larger current range for this effect. It is not yet known if this is a real effect, therefore, the part of the curves that represent the negative resistance are to be taken as tentative rather than final.

2) NASA's specimens have higher normal resistivity values when transition temperatures are reached. Battelle's specimens have much smaller normal-resistivity value when the temperature (critical) is reached.

3) Critical transition temperature range is large for NASA specimens (vary from 4.3K to 14.5K). This could be because of the presence of several phases, each with its own transition temperature. For example, the samples containing tin, show transitions reaching down toward 4°K, the tin transition temperature. In the case of 81NbBr53, the transition stretches upward to 14.5°K, near the transition temperature for the Nb_3Sn compound. Battelle's specimens have smaller critical transition temperature range (vary from 7.2K minimum to 9.4K maximum).

4) The sample (81NbBr53) which was compacted as niobium and bronze powders and then directionally solidified, showed the highest transition temperature and the widest transition range. It also had the highest critical current of the directionally solidified samples. This indicates that both stages (preparation of the ingot, and its later processing) determine the final superconducting properties of the material.

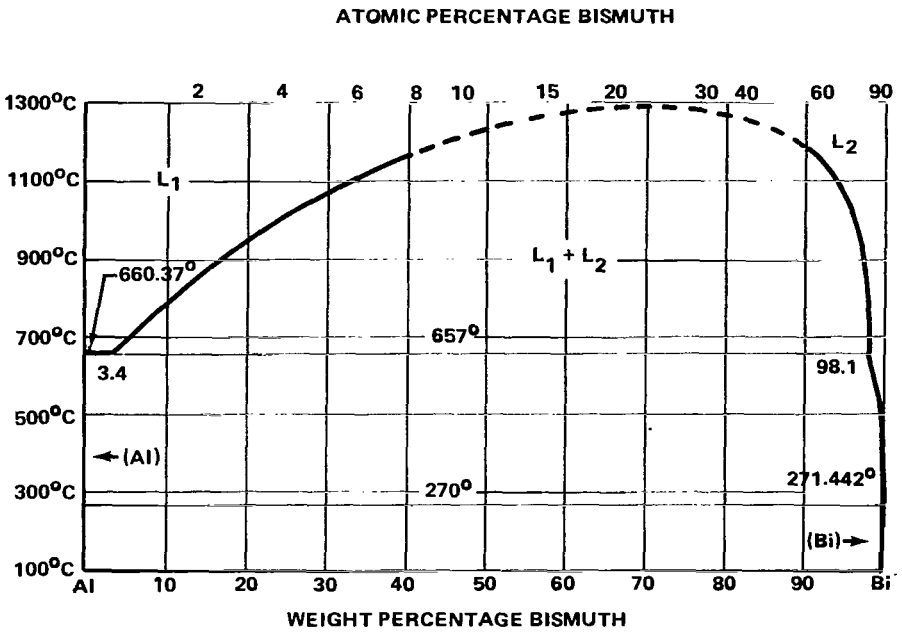

THE ALUMINUM–BISMUTH PHASE DIAGRAM

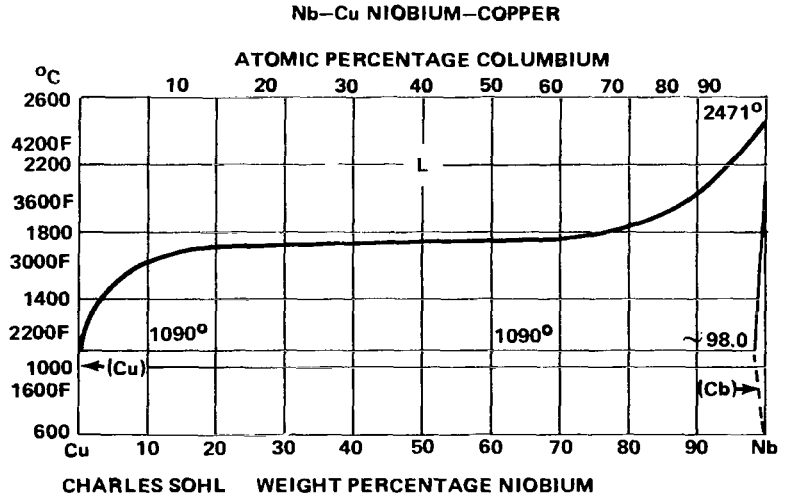

Figure 1. Aluminum bismuth and copper-niobium phase diagrams.

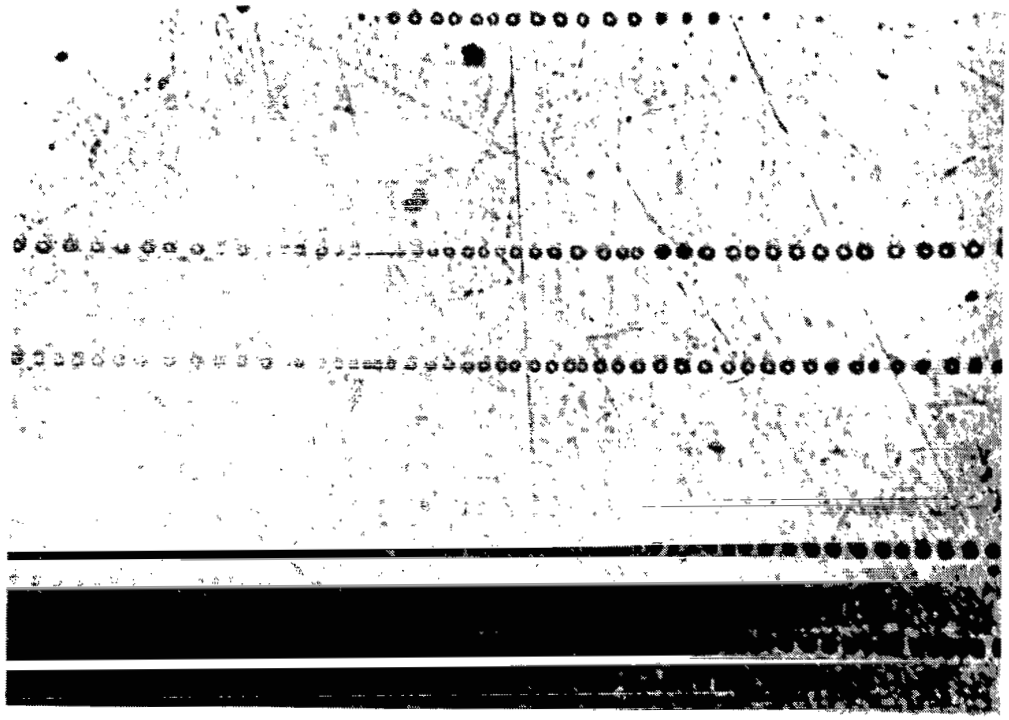

a. Aligned Spheres (200X)

b. Aligned Rods (200X)

Figure 2. Aligned rod and sphere structures on directionally solidified Al-Bi-Fe.

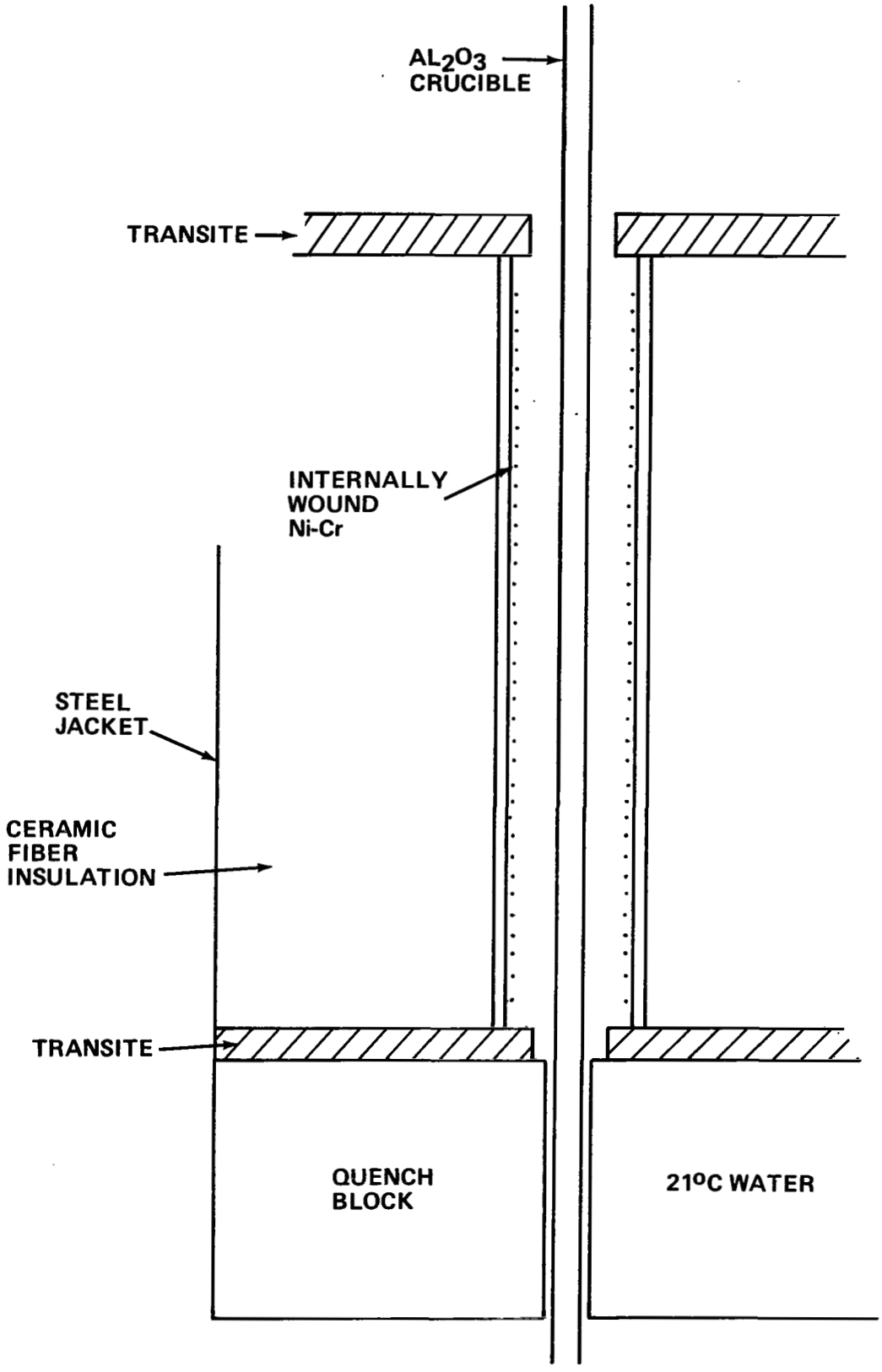

Figure 3. Directional solidification furnace schematic.

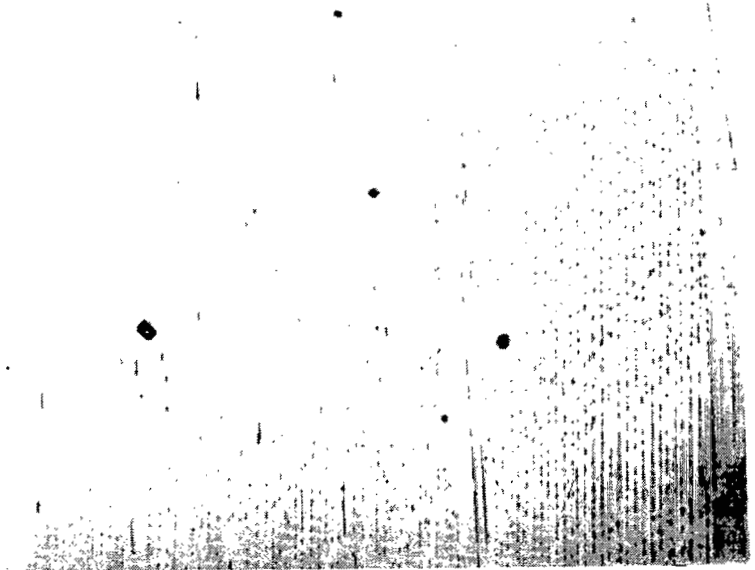

a. 100X

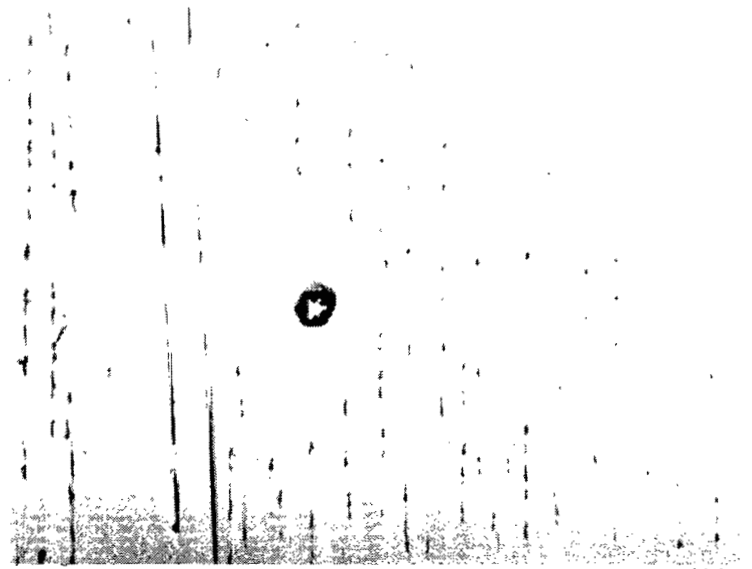

b. 400X

Longitudinal

c. 200X

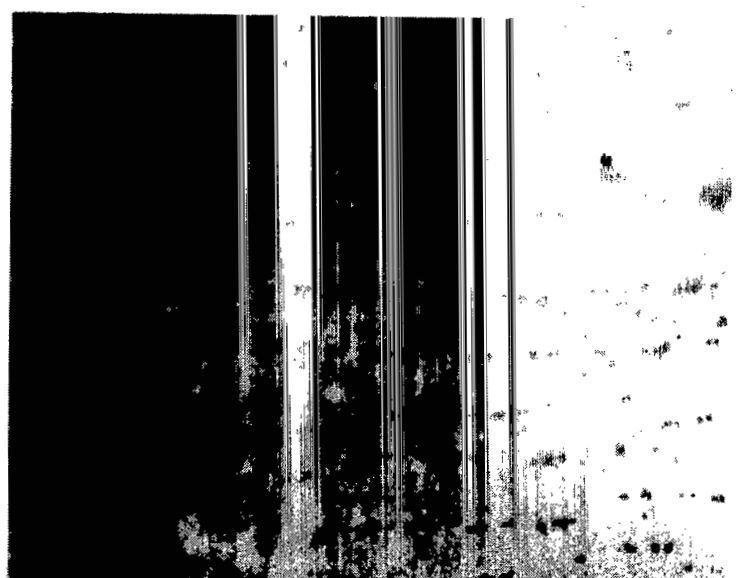

d. 800X

Transverse

Figure 4. Copper-5% niobium-0.25% aluminum alloy directionally solidified at 1200°C set point and 1.7 cm/hr (Spec. 81 CNA41) Waterbury's etchant.

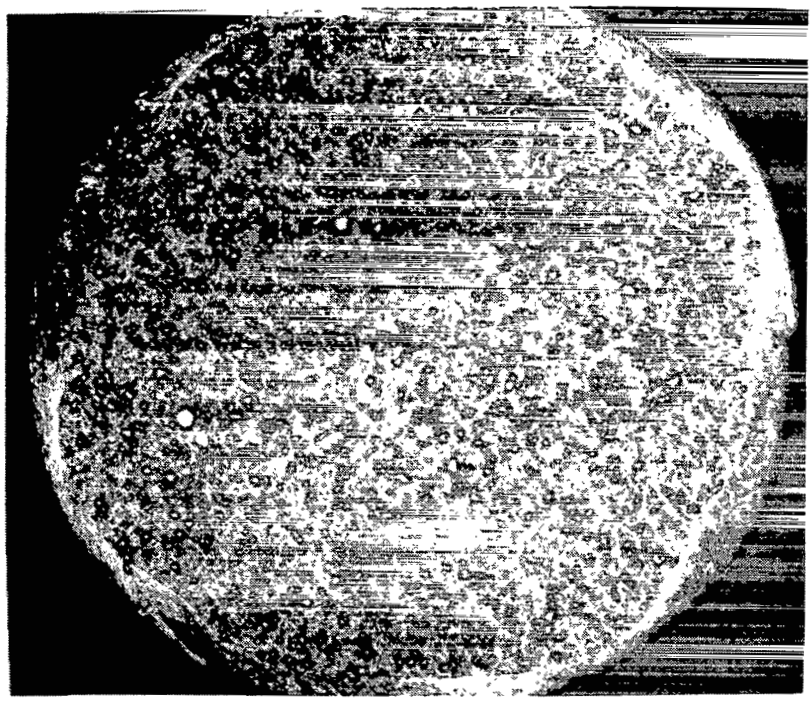

a. Transverse View (45X)

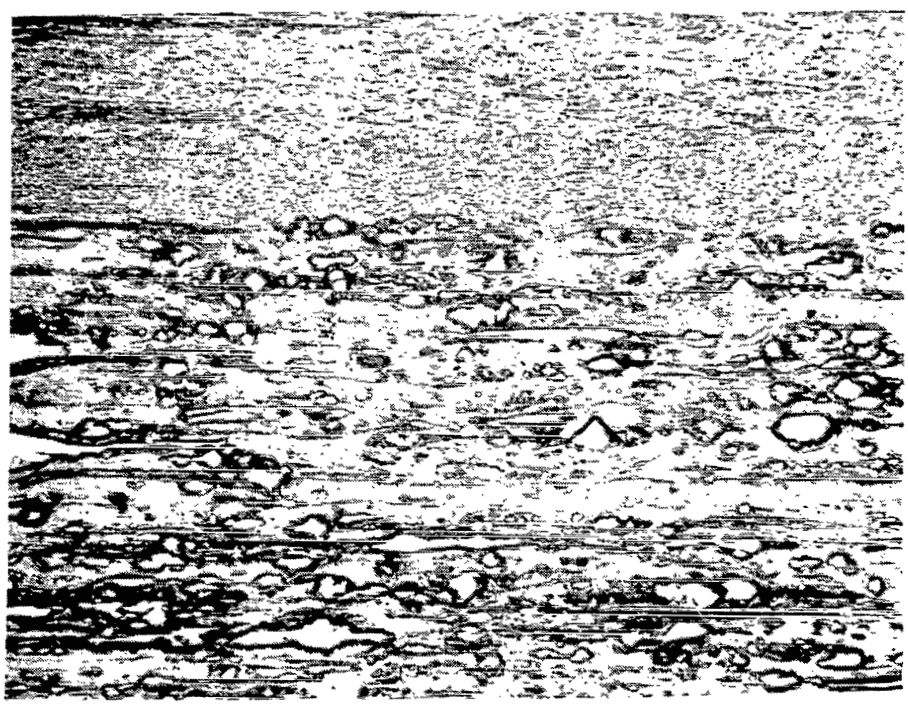

b. Longitudinal View (175X)

Figure 5. Niobium in bronze matrix (Cu-10%Sn), prepared by powder metallurgy, canned in pure copper, extruded and rolled. (Specimen NbBr 169 (C)T) Waterbury's etchant.

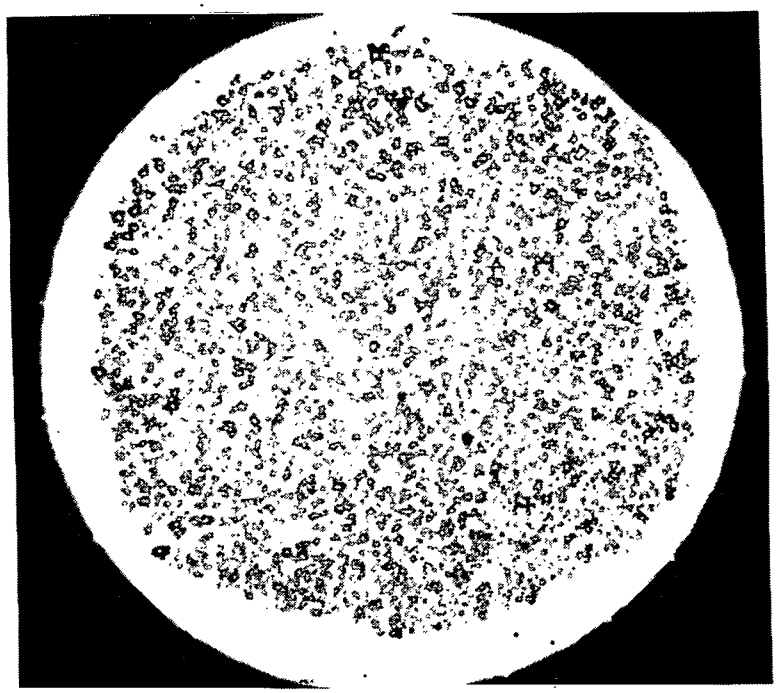

a. Transverse View (37.5X)

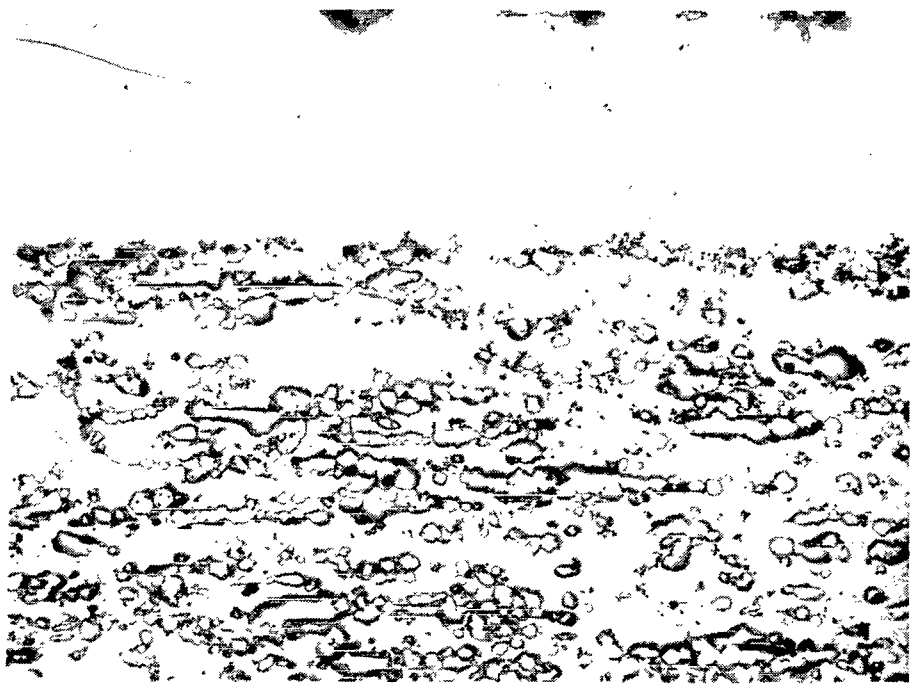

b. Longitudinal View (180X)

Figure 6. NbBr 169 (C)T after directional solidification at 1200°C and 4.23 cm/hr.

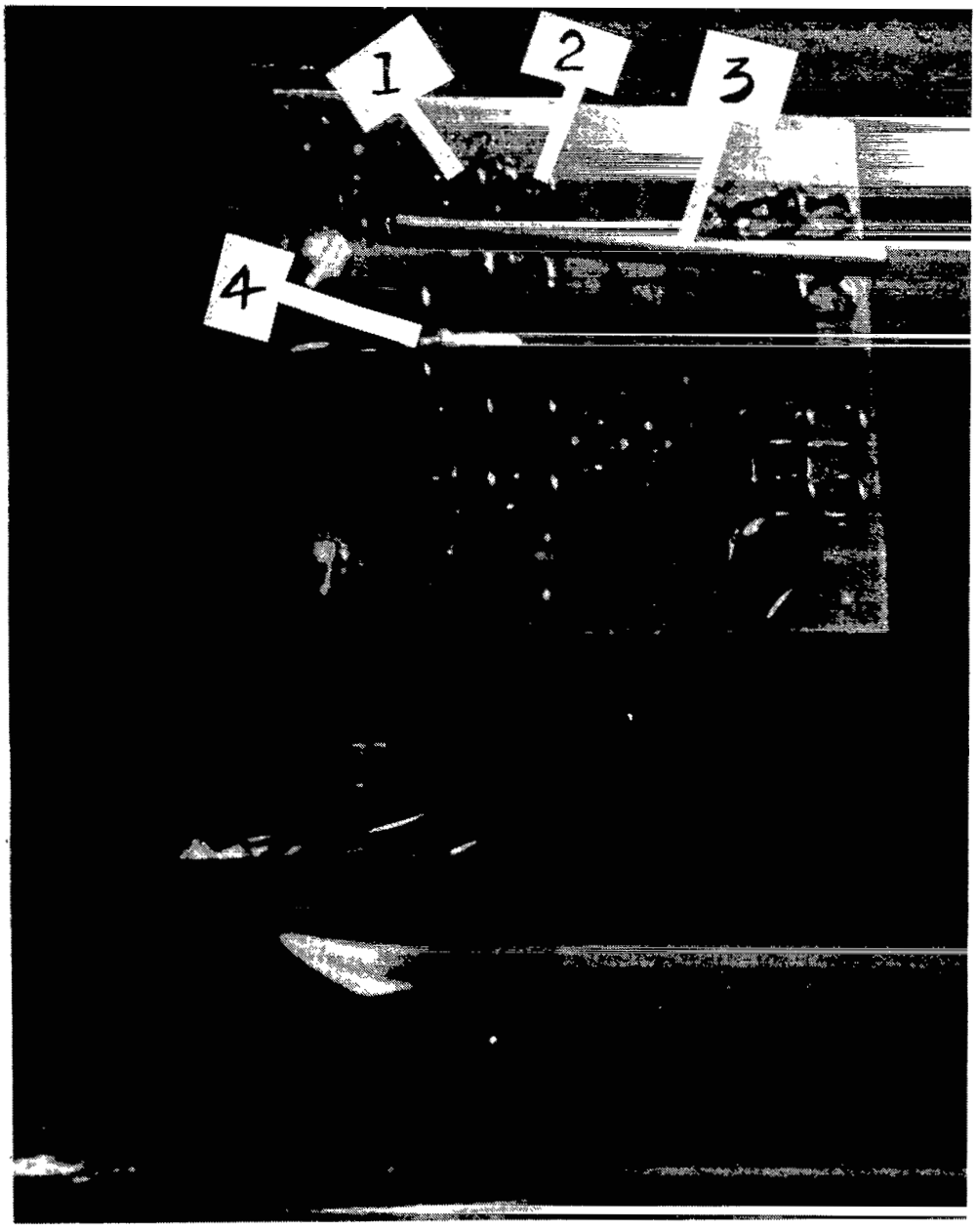

SAMPLE HOLDER AND ITS COMPONENTS

1. Current Probe
2. Voltage Probe
3. Sample
4. Resistance Thermometer

Figure 7. Specimen holder for superconductivity measurement.

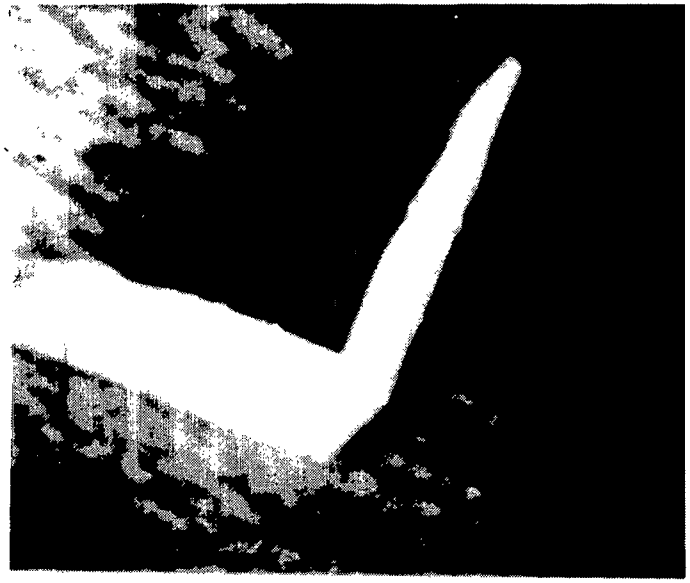

a. 4000X

b. 1500X

c. 10,000X

d. 1000X

Figure 8. SEM photomicrographs of aligned Niobium compound (a, b, and c) and Niobium Dendrite (d). Waterbury's etchant.

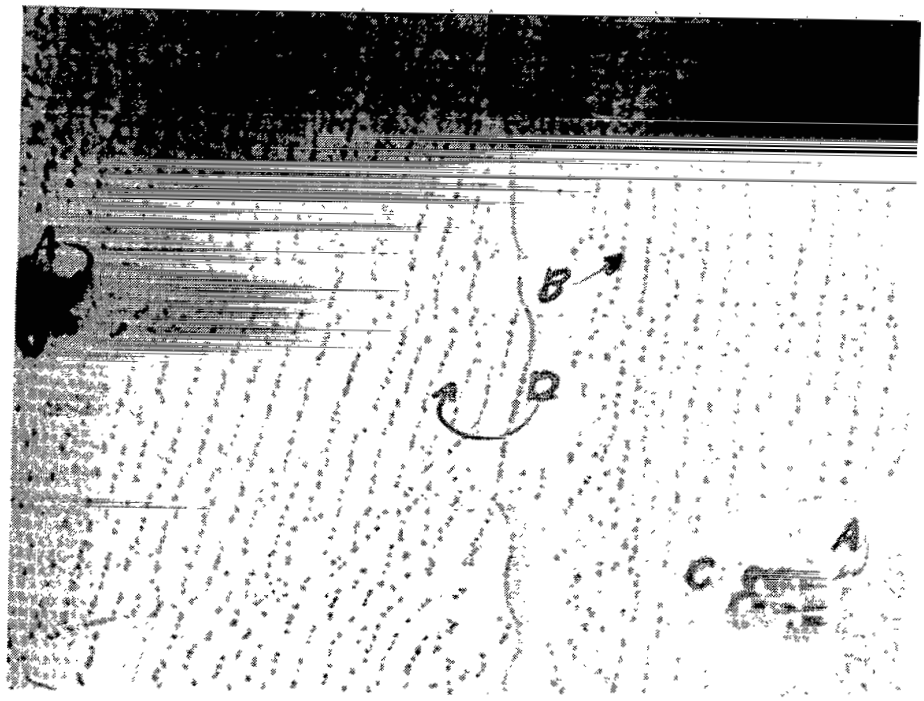

Figure 9. Specimen 81CNA42 directionally solidified at 1200°C and 4.23 cm/hr. Electron microprobe analyses were made in the representative areas indicated by the letters. Transverse Cross Section. Waterbury's etch.

a. 15Kv b. 20Kv

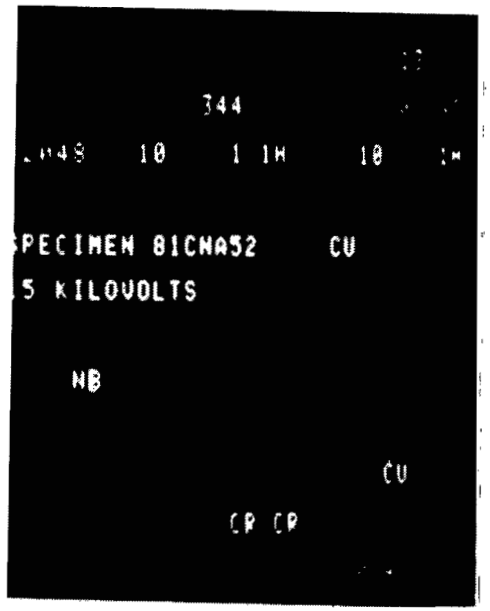

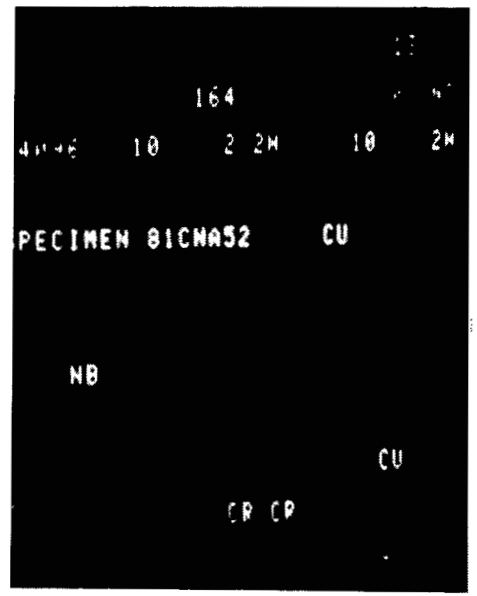

Fine Rods

c. Right Angle d. Rectangular

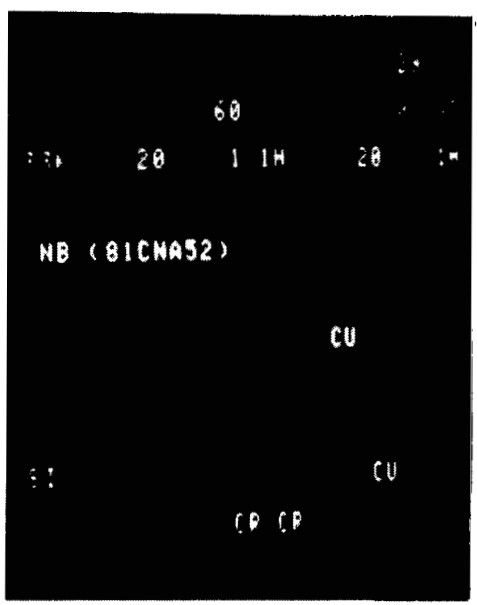

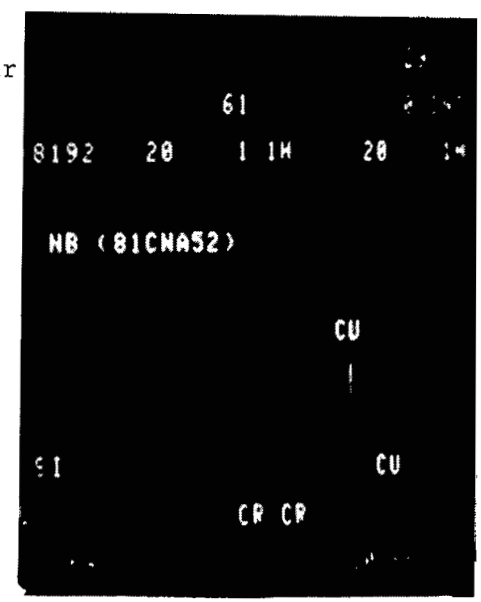

Coarse Rods

Figure 10. Kevex spectra of specimen 71CNA52 directionally solidified at 1200°C and 4.39 cm/hr.

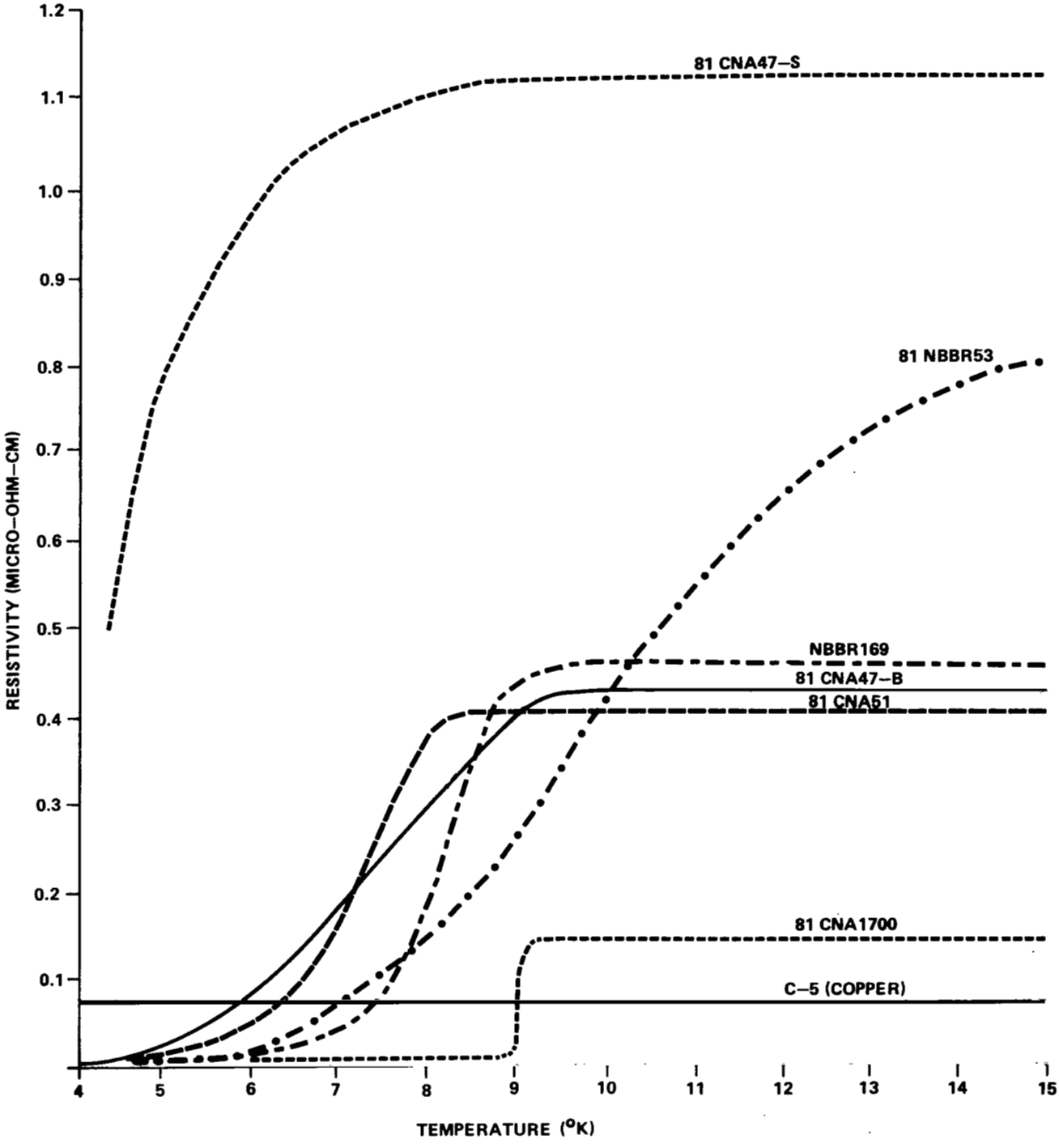

Figure 11. Electrical resistivity as a function of temperature.

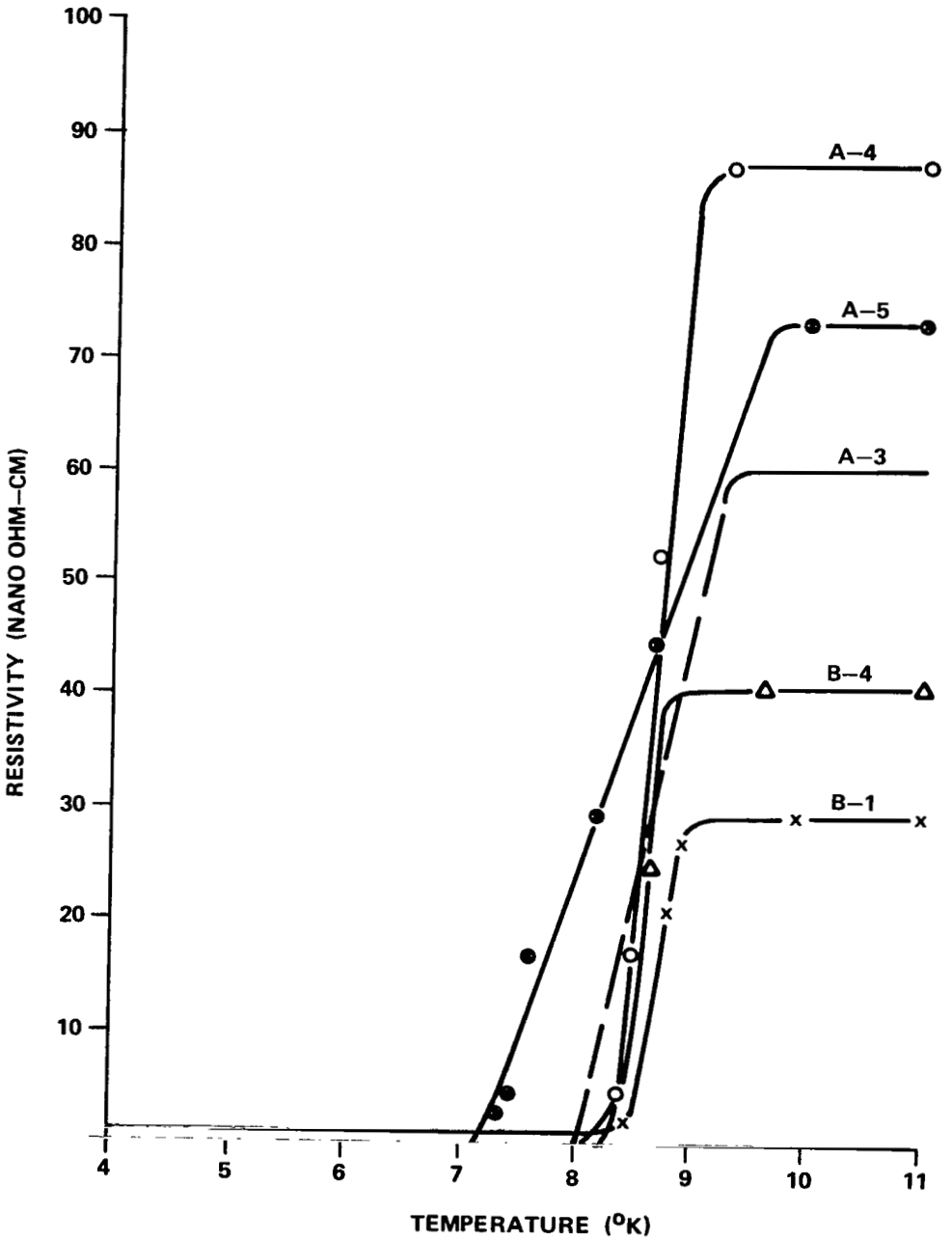

Figure 12. Electrical resistivity as a function of temperature for the five Battelle specimens.

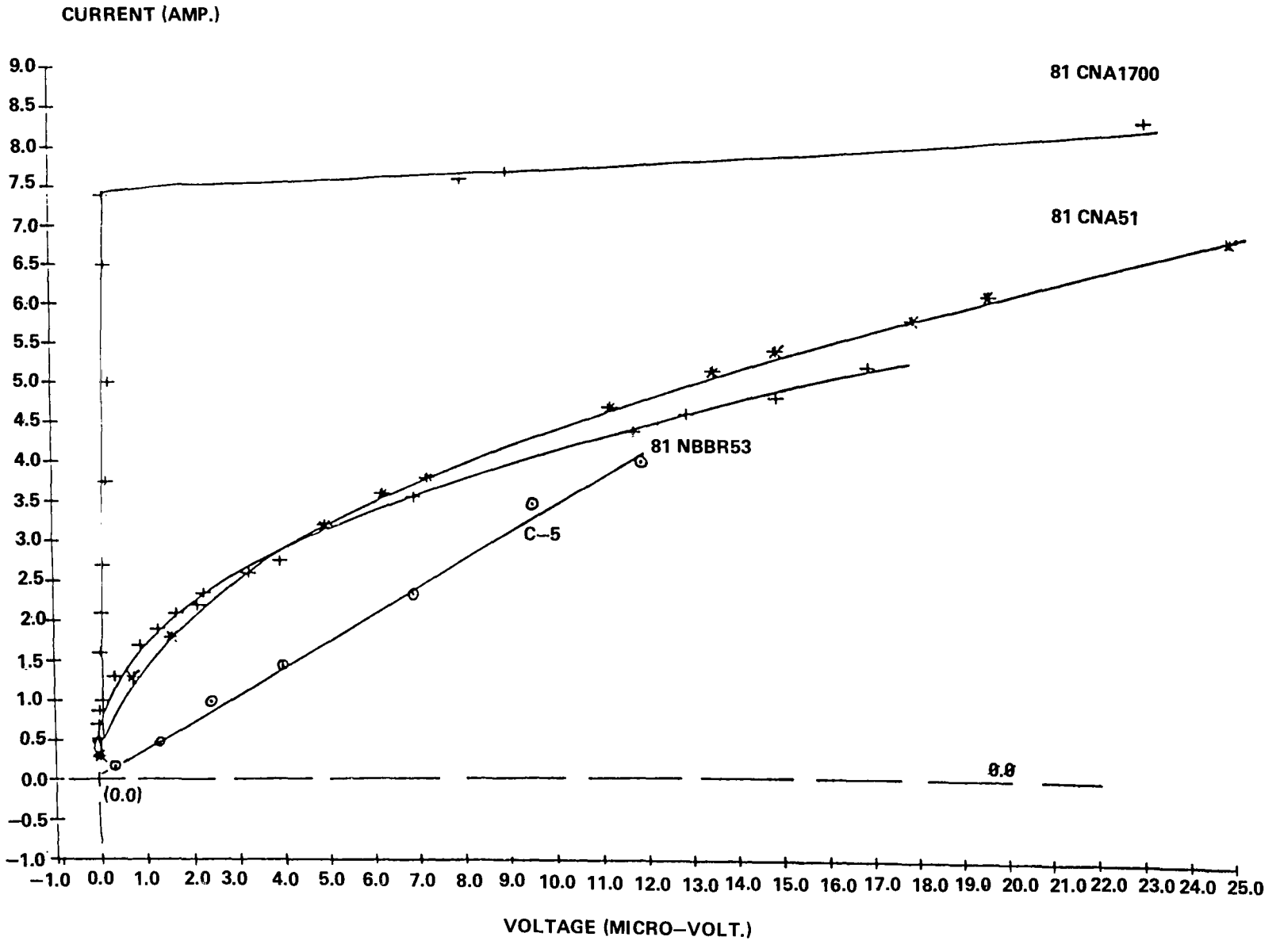

Figure 13. Current-voltage characteristics of four testing specimens.

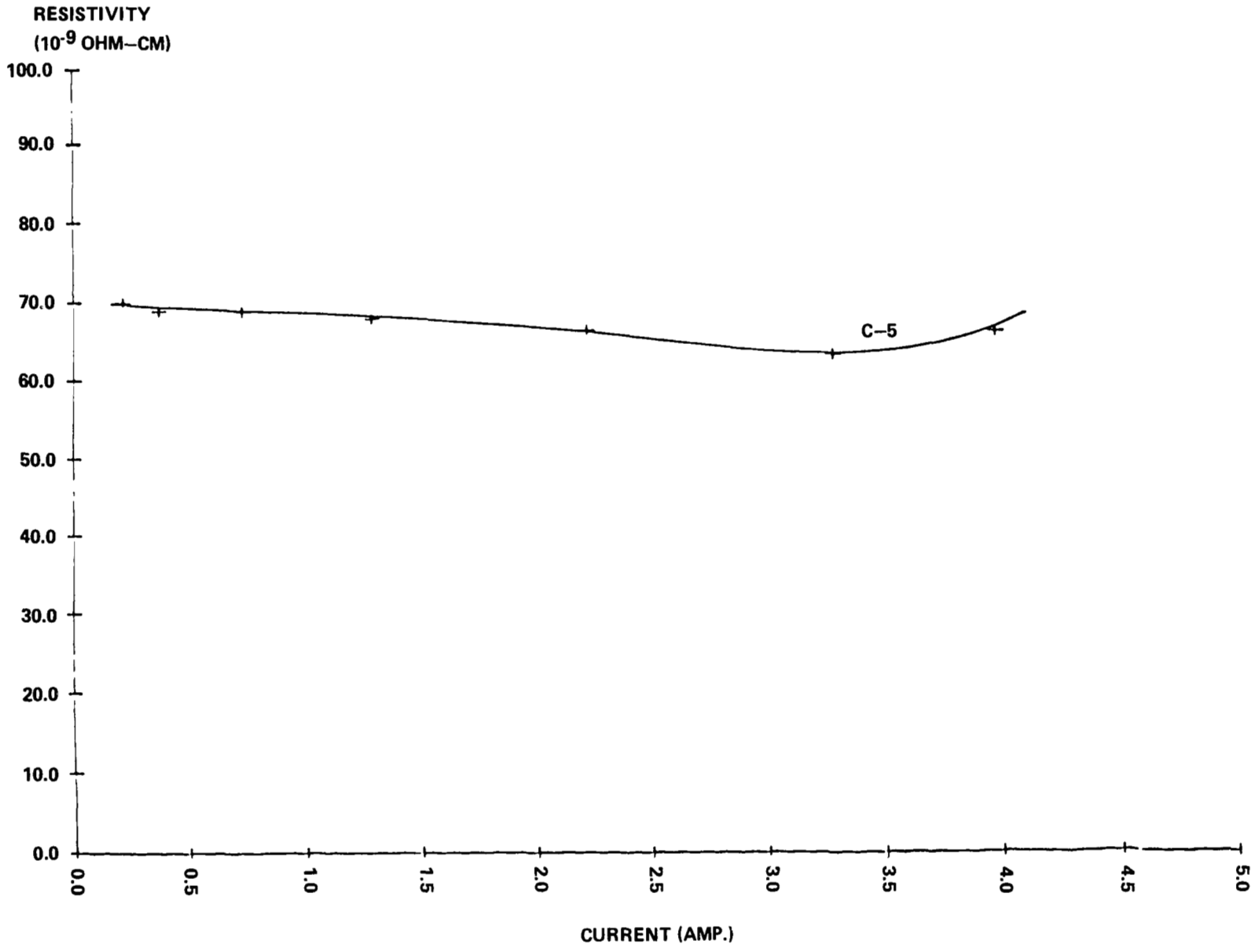

Figure 14. Resistivity-current characteristics for sample C-5 (99.9 percent pure copper) (T = 4.3K).

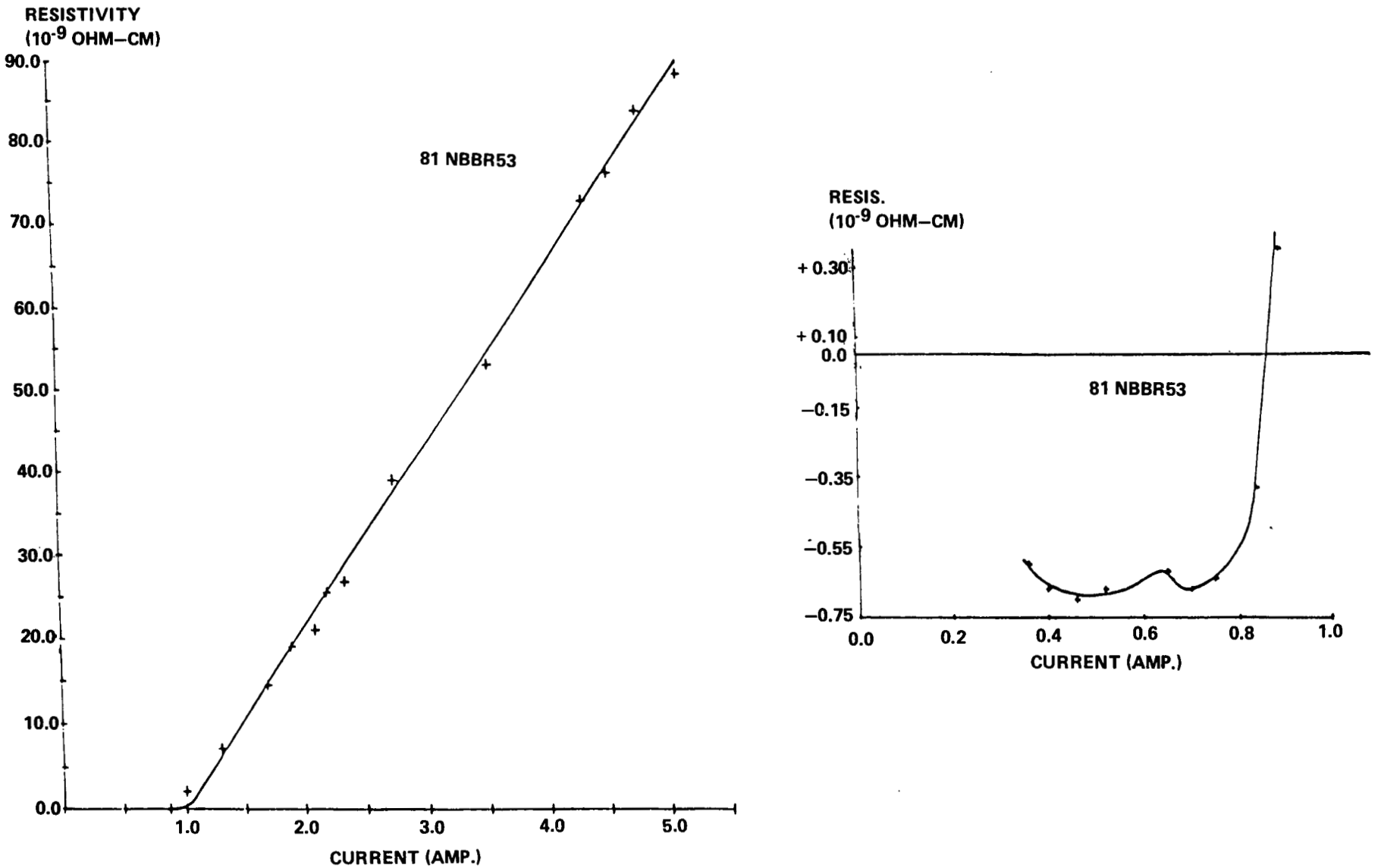

Figure 15. Resistivity-current characteristics of specimen 81NbBr53. Note that when the applied current is greater than 0.8 A, the sample shows positive resistance.

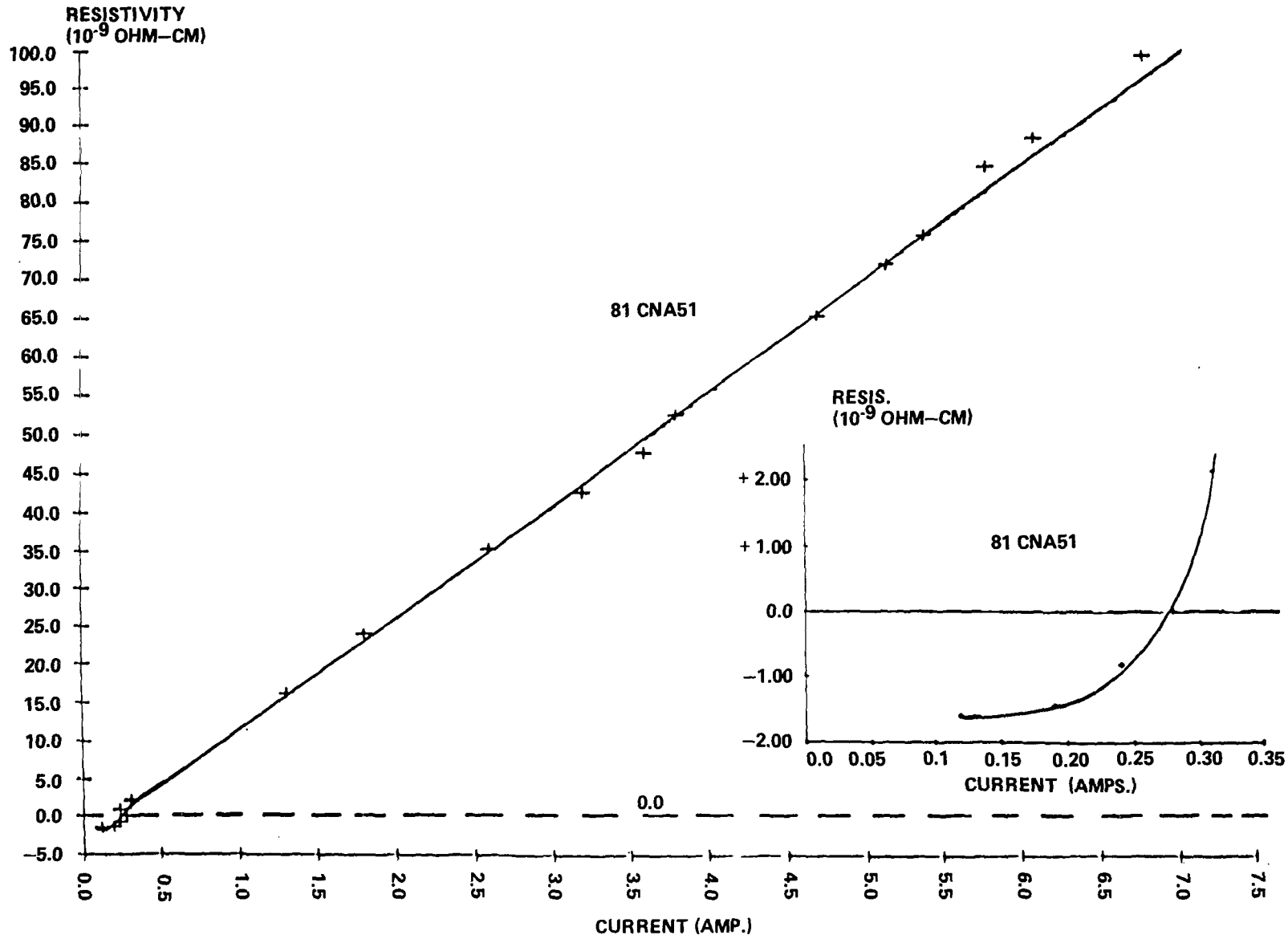

Figure 16. Resistivity-current characteristics of specimen 81CNA51.

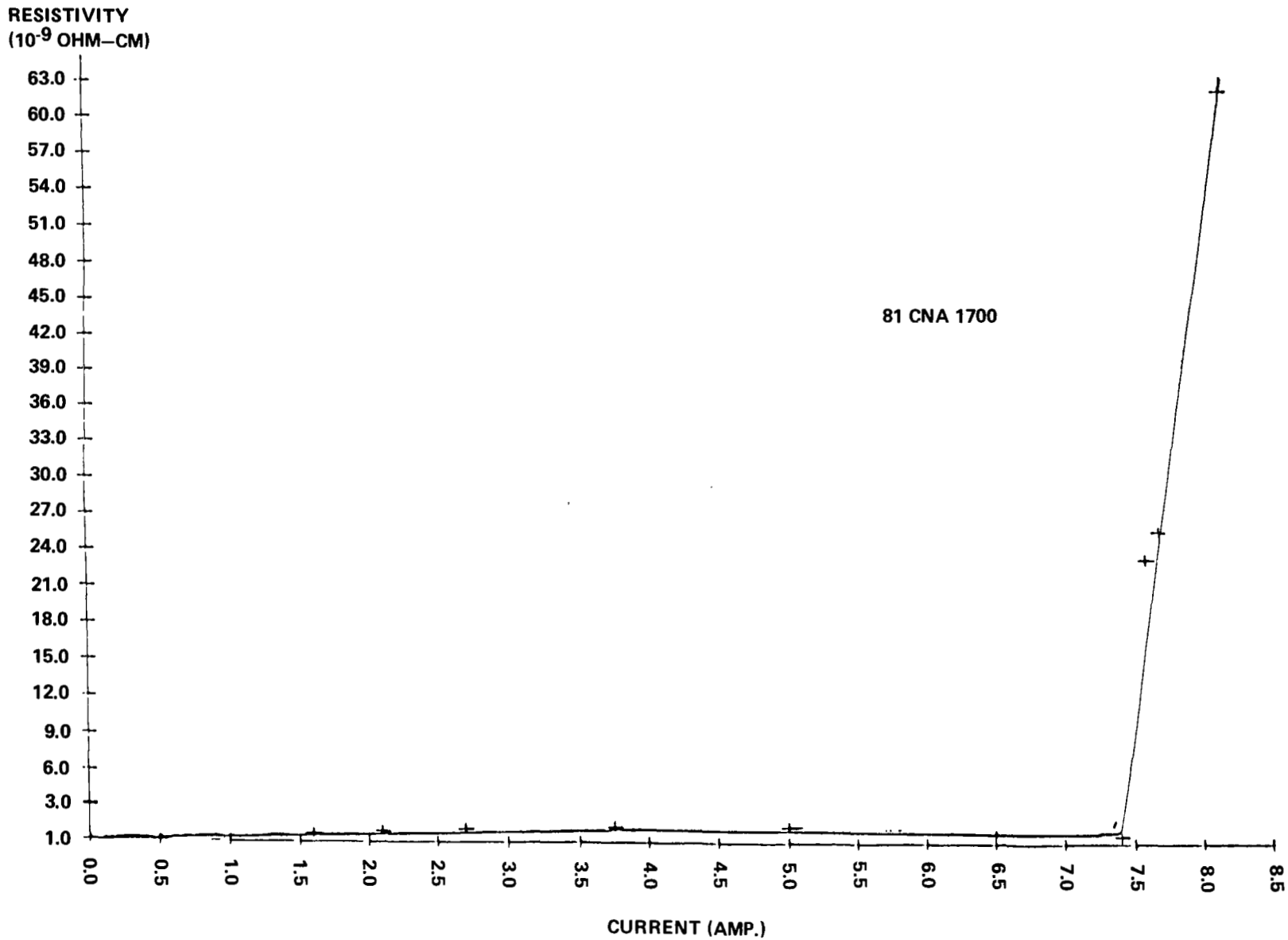

Figure 17. Resistivity-current characteristics for specimen 81CNA1700.

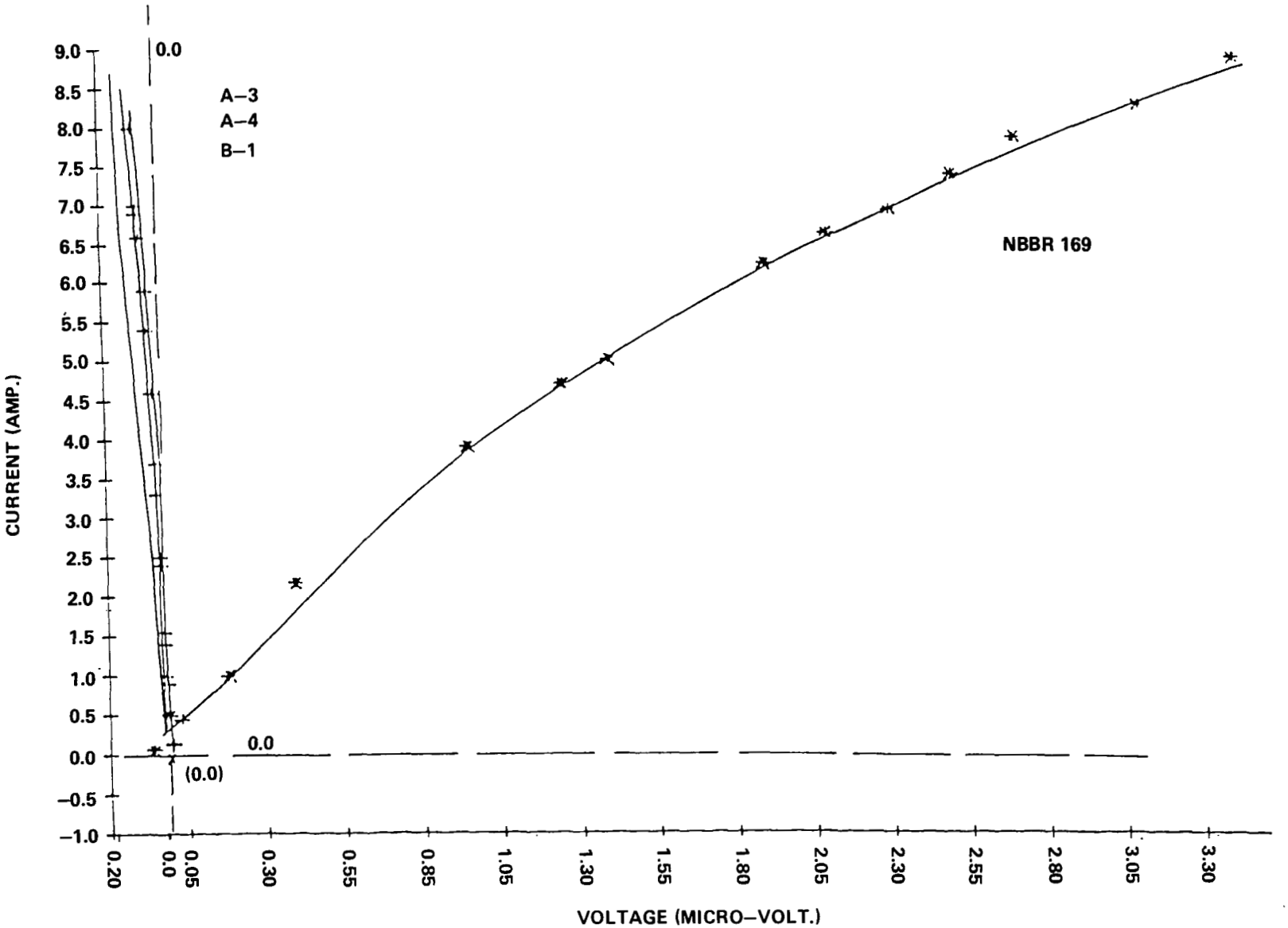

Figure 18. Current-voltage characteristics for specimens A-3, A-4, B-1, and NbBr 169 at T = 4.3K.

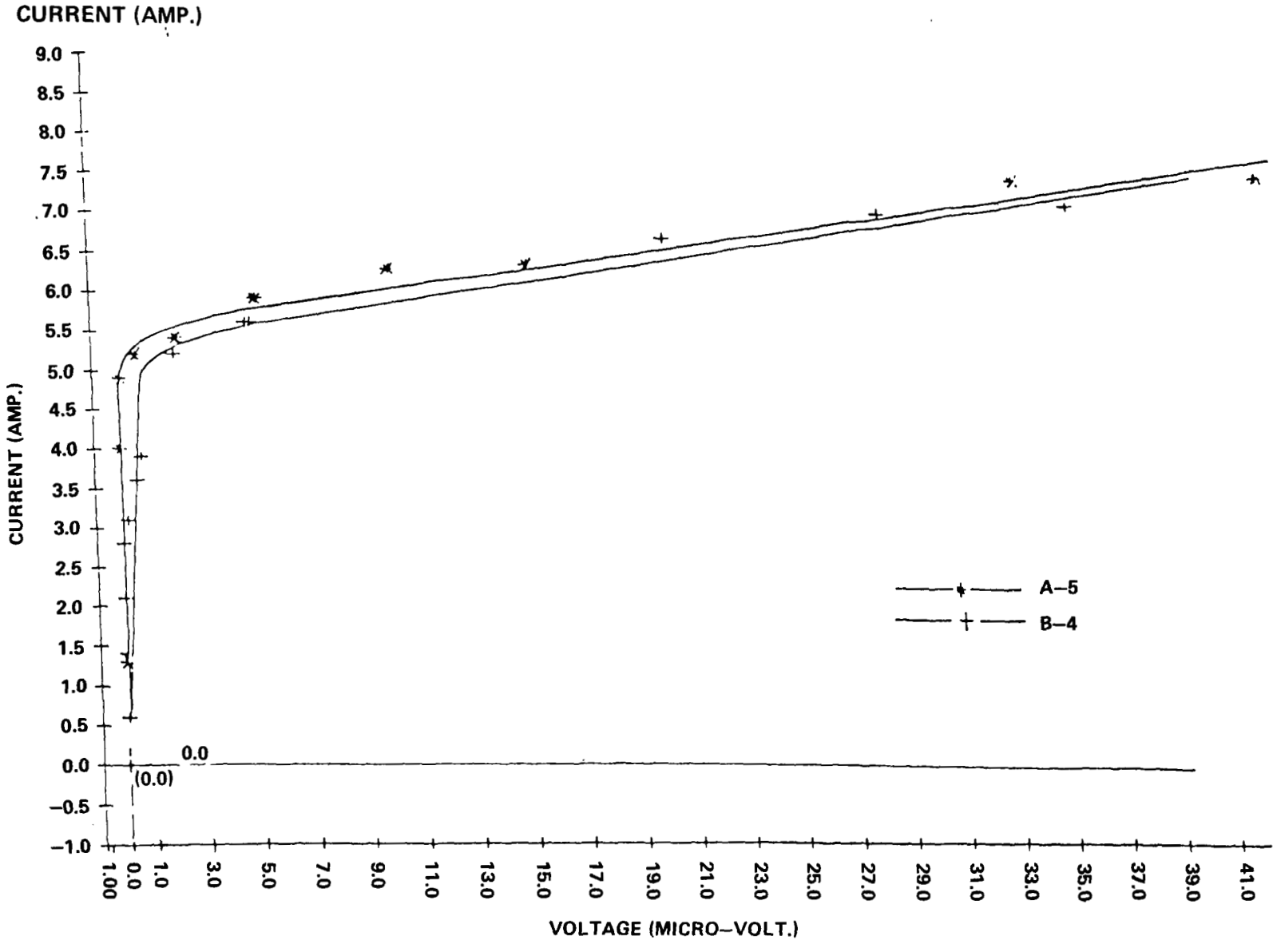

Figure 19a. Current-voltage characteristics of specimens A-5, B-4, T = 4.3K.

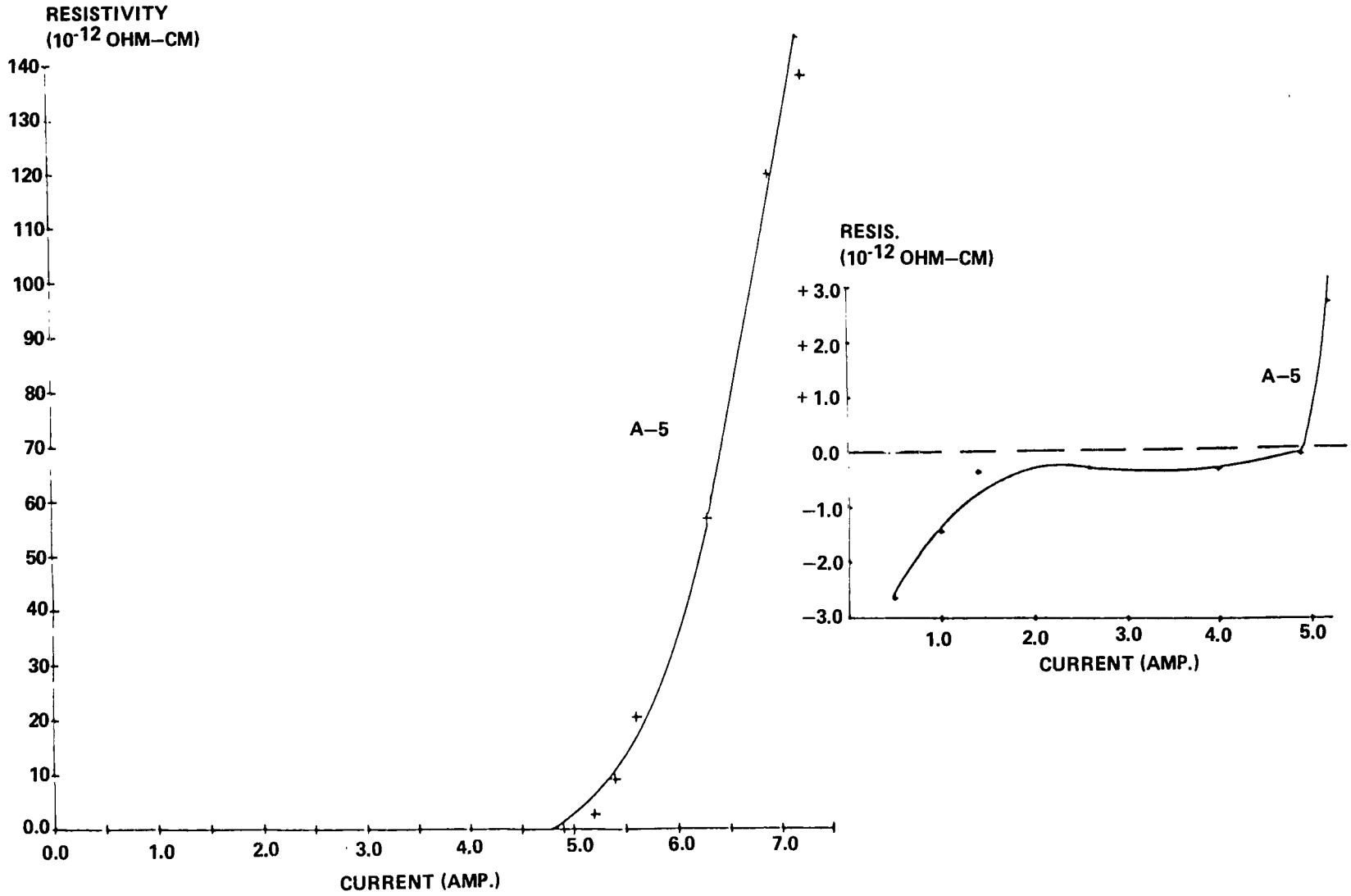

Figure 19b. Resistivity-current characteristics for A-5 at 4.3K.

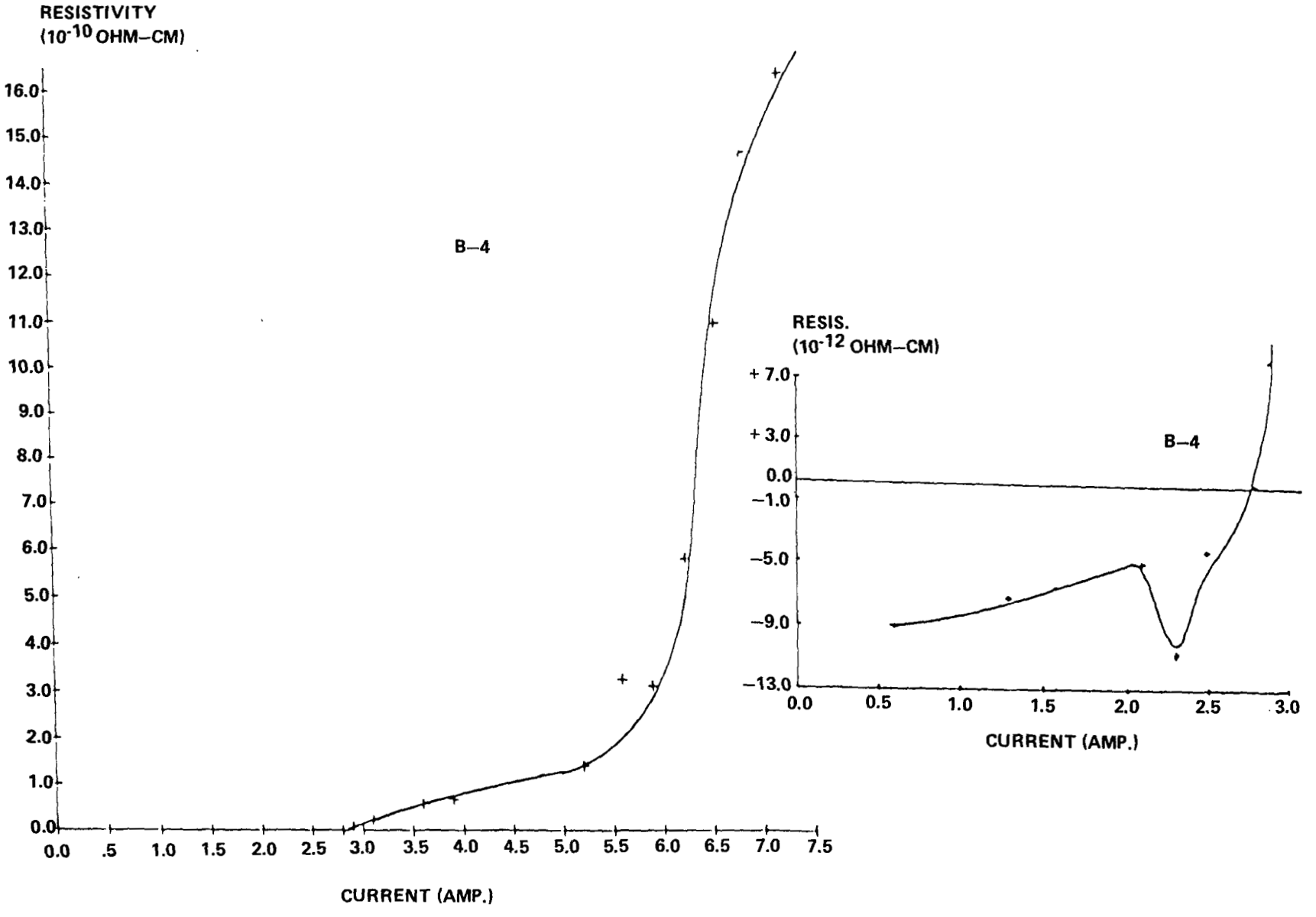

Figure 19c. Resistivity-current characteristics of specimen B-4 at 4.3K.

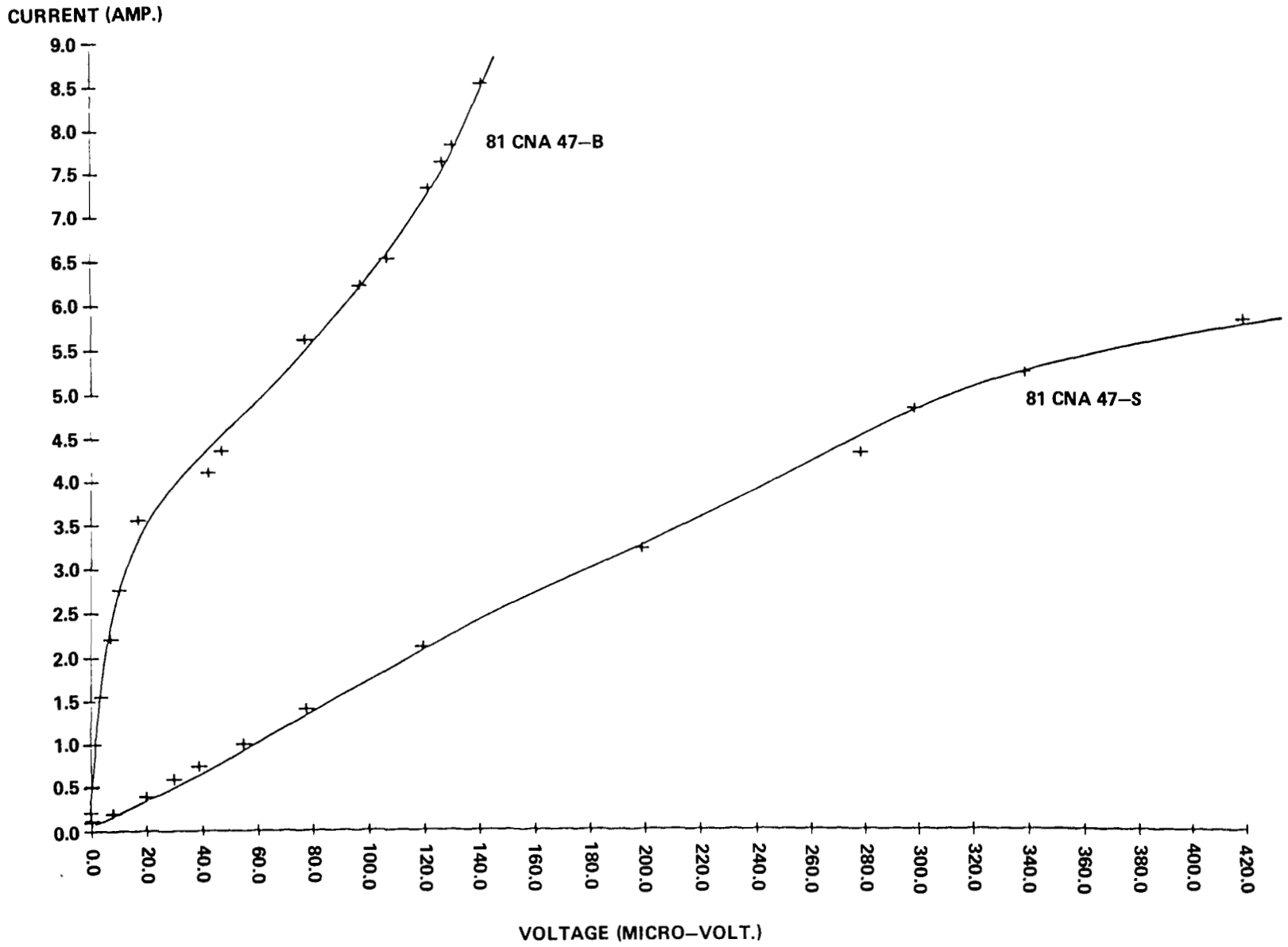

Figure 20. Current-voltage characteristics of specimens 81CNA47-B and 81CNA47-S at 4.3K.

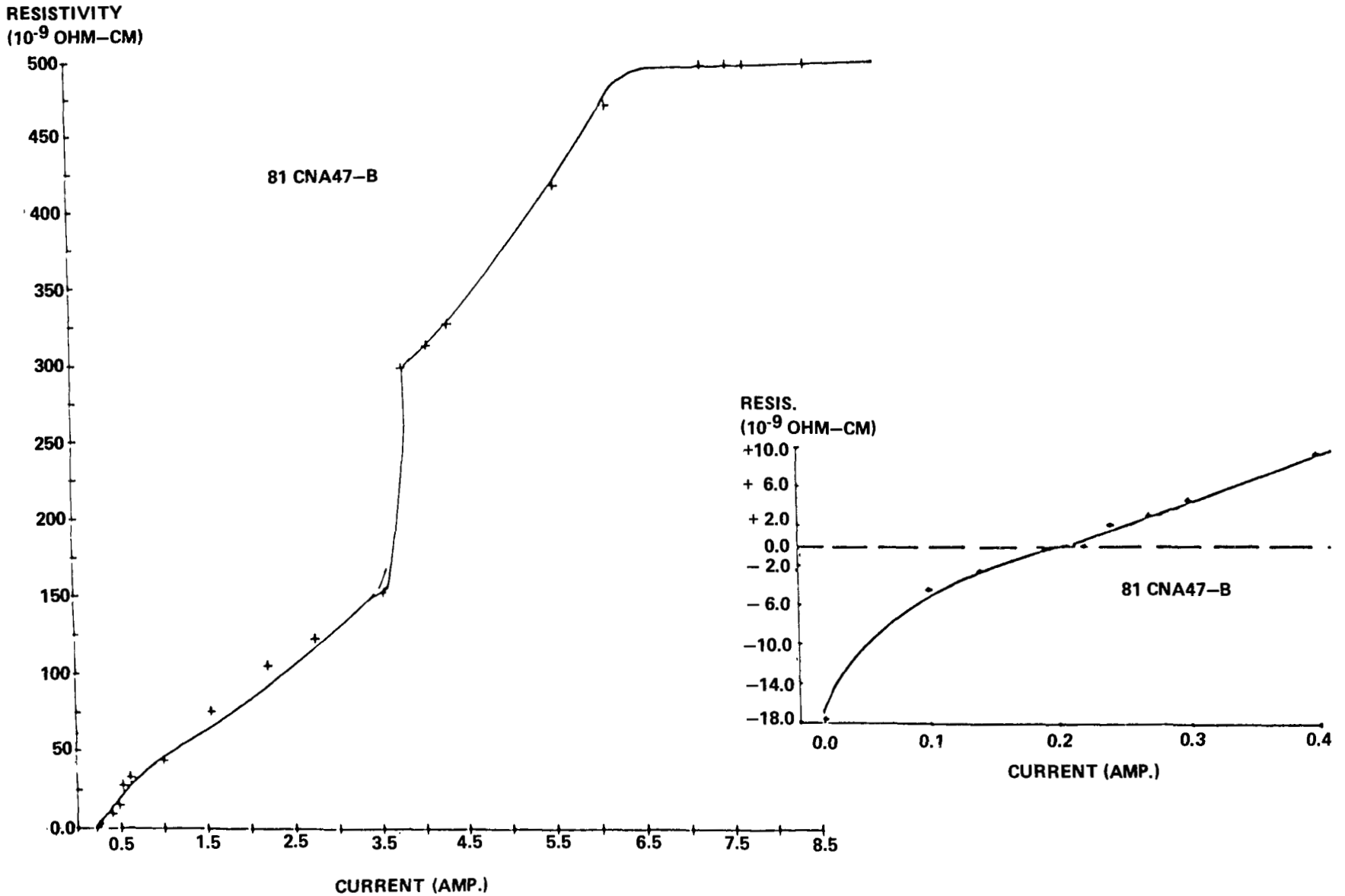

Figure 21. Resistivity-current relations of specimen 81CNA47-B at 4.3K.

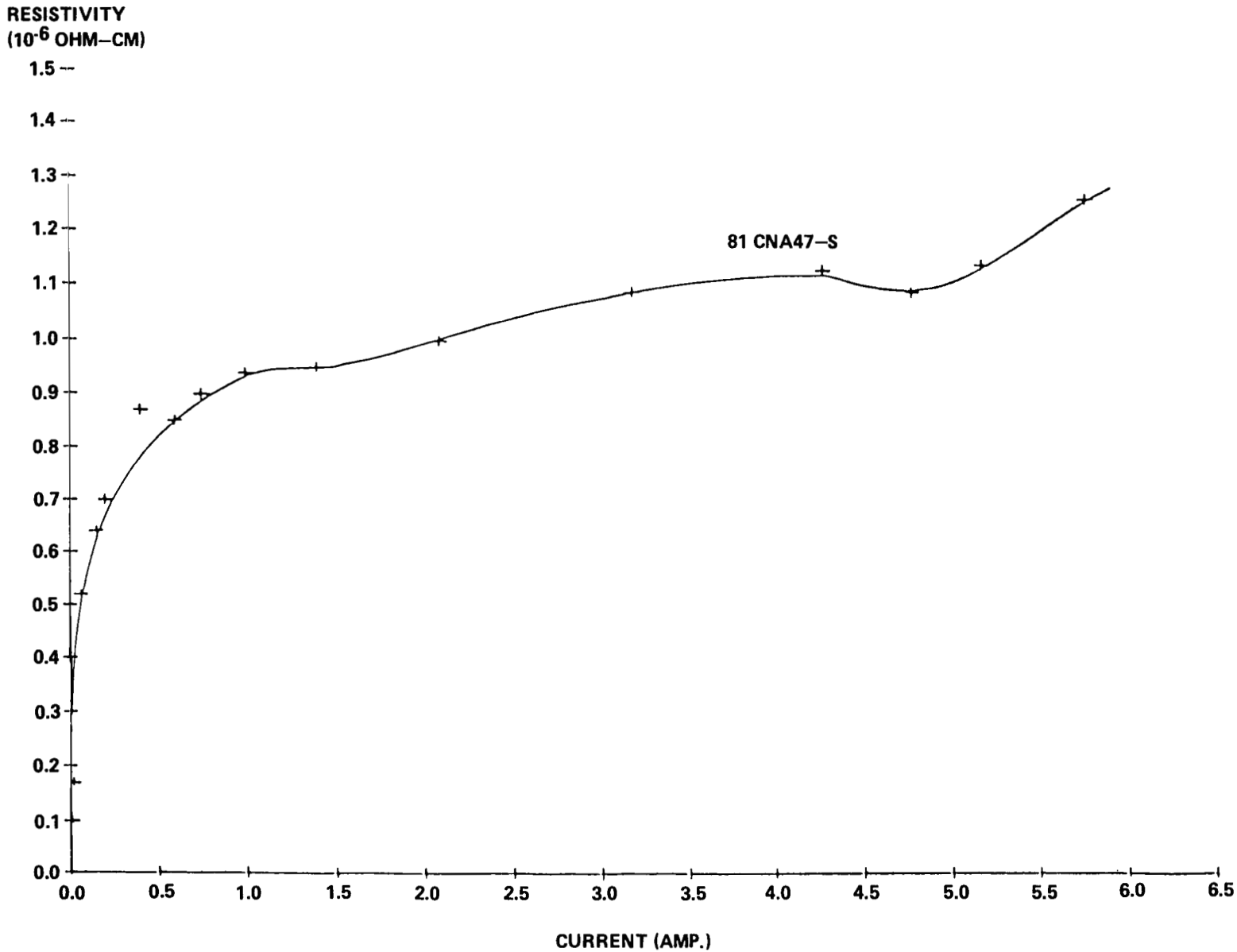

Figure 22. Resistivity-current relations of sample 81CNA47-S at 4.3K.

TABLE 1. CROSS SECTIONAL AREAS AND SPECIMEN HISTORIES

Sample No.	Cross Sectional Area (cm^2)	Alloy and Condition
CNA 1700	0.0353	Cu-5%. As rolled
NbBr 169	0.0370	Cu-19.5%Nb-8.5%Sn. Powder Met. Alloy from Battelle, Extruded and cold rolled.
81NbBr53	0.043	Same as specimen NbBr 169, except Directionally Solidified
81CNA 51	0.044	Cu-5%Nb-0.25%Al. Directionally Solidified.
81CNA47-S	0.011	Cu-5%Nb-0.25%Al. Directionally Solidified, Cold Rolled and Tin Diffused. (2.4% Sn)
81CNA47-B	0.047	Cu-5%Nb-0.25%Al. Directionally Solidified and Tin Diffused. (3.0%Sn)
A-3	$1.6\ 10^{-3}$	Cu-Nb Alloy
A-4	2.54×10^{-4}	Cu-Nb Alloy
A-5	3.84×10^{-5}	Cu-Nb Alloy
B-1	0.012	Cu-Nb Alloy
B-4	5.83×10^{-4}	Cu-Nb Alloy
C-5	0.0353	Copper 99. %

TABLE 2. PROCEDURES FOR PREPARING SAMPLES FOR SUPERCONDUCTIVITY MEASUREMENTS

CNA-1700; Cu-5%Nb-.25%Al. Alloy was melted at 1700°C. Casting was then cold rolled with intermediate anneals, from 0.50 inch to .083 inch rod.

NbBr-169; Cu-19.5%Nb-8.5%Sn. Alloy was prepared by powder metallurgy Niobium and bronze powders compacted, placed in copper tube and then was extruded to 0.21 inch diameter rod. The rod was further reduced to .083 inch by cold rolling.

81NbBr53; Alloy is same as NbBr-169. It was directionally solidified at 1200°C at a rate of 4.39 cm/hr.

81CNA 51; Cu-5%Nb-0.25%Al. Sample was directionally solidified from rod of CNA-1700 at 1200°C and growth rate of 4.36 cm/hr.

81CNA47-S; Cu-5%Nb-0.25%Al-2.4%Sn & 81CNA47-B; Cu-5%Nb-0.25%Al-3.0%Sn. These samples were directionally solidified similar to 81CNA51. Then 81CNA47-S was cold rolled to a diameter of .042 inch for a reduction in area of 80%. Both samples were hot dipped in pure tin and sealed in vapor tubing under a partial pressure of argon, after examination. The tin was diffused into the samples by heating initially at 200°C and then raising the temperature to 650°C. Total heating time was approximately 72 hours.

A-3, A-4, A-5, B-1 and B-4; Copper-niobium composites. These samples were prepared at Battelle by co-extruding niobium contained in a copper can. The extension was then reduced by rolling and drawing through wire dies into wires from .003 inch to .048 inch in diameter.

C-5, Pure Copper. This sample was obtained from melted and rolled copper.

TABLE 3. MICROPROBE ANALYSIS OF SPECIMEN 81CNA42

Area	Element, %		
	Cu	Al	Nb
A - "Rosettes"	5.12, 3.26	2.54, 2.31	92.16, 94.03
B - Small "Rods"	98.79	.17	.06
C - Area Between A & B	99.83	.11	---
D - Area Between Small Precipitates	99.80	.10	.09

TABLE 4. EDAX ANALYSIS OF SPECIMEN 81CNA41

Area	Element, %		
	Cu	Al	Nb
A - Large Stringer	7.50	3.33	88.66
B - Small Rods	77.84	----	21.66
C - Small Rods	77.72	----	21.78
D - Small Rods	97.39	----	2.11
E - Small Rods	64.25	----	35.25

TABLE 5. RESISTIVITY-TEMPERATURE CHARACTERISTICS FOR TWELVE TESTED SPECIMENS

Sample No.	Current Density (A/cm^2)	Transition Temp. Range (K)	Normal Resistivity (Ohm-cm)
NBBR 169	7	5.5 to 9.5	0.45×10^{-6}
81CNA1700	5.3	8.5 to 9.3	0.14×10^{-6}
81NBBR 51	11.4	4.3 to 8.5	0.40×10^{-6}
81NBBR 53	2.3	5.5 to 14.5	8.0×10^{-6}
81CNA47-S	8.8	4.3 to 8.0	1.1×10^{-6}
81CNA47-B	5.3	4.3 to 9.5	0.43×10^{-6}
A-3	62.5	8.0 to 9.4	0.6×10^{-7}
A-4	400	8.2 to 9.3	0.86×10^{-7}
A-5	2604	7.2 to 9.8	0.72×10^{-7}
B-1	8.3	8.5 to 9.2	0.29×10^{-7}
B-4	175	8.0 to 9.0	0.41×10^{-7}
C-5 (99.5%Cu)	14.2	NONE	NONE

TABLE 6. RESISTIVITY-CURRENT CHARACTERISTICS OF THE TWELVE SPECIMENS

Sample No.	Critical Current (A/cm^2)
81CNA 1700	210
NBBR 169	3.50
81NBBR 51	6.37
81NBBR 53	19
81CNA47-S	None
81CNA47-B	4.70
A-3	??
A-4	??
A-5	125,000
B-1	??
B-4	4460
C-5	None

REFERENCES

1. Reger, J. L.: Study on Processing Immiscible Materials in Zero Gravity. Interim Report, May 1973, NAS8-28267.

2. Hansen, Max: Constitution of Binary Alloys. McGraw Hill Book Company, Inc., 1958.

3. Johnston, M. H., Parr, R. A., and McClure, J. C.: U. S. Patent No. 4,198,232.

4. Parr, R. A. and Johnston, M. H.: Metallurgical Transaction, Vol, 9A, 1978, p. 1825.

5. Johnston, M. H. and Parr, R. A.: Conference on In Situ Composites-III. Ginn Custom Publishing, J. L. Walter, M. F. Gigliotti, B. F. Oliver, and H. Bibring (editors), 1979, p. 49.

6. Hancox, R.: IEEE Trans. on Magnetism. Vol. MAG-4, 1968, p. 486.

7. Organic Superconductors, Scientific American Magazine, July 1982.

8. Alterovitz, S. A., Woolarm, J. A., and Collings, E. W.: IEEE Transactions on Magnetics. Vol. Mag. 15, No. 1, January 1979, p. 404.

9. Solymar, L.: Superconductive Tunnelling and Applications. John Wiley and Sons, Inc., 1972.

10. Kim, Y. B. and Stephen, M. J.: Superconductivity. Marcel Dekker, Inc., New York, R. D. Parks (editor), 1969, p. 1141.

11. Davies, R. O. (editor): Proceedings of the 9th International Conference on Low Temperature Physics. Butterworths, London, 1963.

12. Blatt, F. J., Schroeder, P. A., Foiles, C. L., and Grieg, D.: Thermoelectric Power of Metals. Plenum Press, New York, 1976.

13. Fiory, A. T. and Serin, B.: Observation of a "Peltier" Effect in a Type II Superconductor. Phys. Rev. Let., Vol. 16, No. 8, 1966, p. 308.

1. REPORT NO.	2. GOVERNMENT ACCESSION NO.	3. RECIPIENT'S CATALOG NO.
NASA TP-2144		

4. TITLE AND SUBTITLE

A Study of Production of Miscibility Gap Alloys With Controlled Structures

5. REPORT DATE
March 1983

6. PERFORMING ORGANIZATION CODE

7. AUTHOR(S)

R. A. Parr, M. H. Johnston, J. A. Burka, J. H. Davis, and J. A. Lee

8. PERFORMING ORGANIZATION REPORT #

9. PERFORMING ORGANIZATION NAME AND ADDRESS

George C. Marshall Space Flight Center
Marshall Space Flight Center, Alabama 35812

10. WORK UNIT NO.
M-406

11. CONTRACT OR GRANT NO.

13. TYPE OF REPORT & PERIOD COVERED

Technical Paper

12. SPONSORING AGENCY NAME AND ADDRESS

National Aeronautics and Space Administration
Washington, D.C. 20546

14. SPONSORING AGENCY CODE

15. SUPPLEMENTARY NOTES

Prepared by Materials and Processes Laboratory, Science and Engineering Directorate.

16. ABSTRACT

Composite materials were directionally solidified using a new technique to align the constituents longitudinally along the length of the specimen. In some instances a tin coating was applied and diffused into the sample to form a high transition temperature superconducting phase. The superconducting properties were measured and compared with the properties obtained for powder composites and re-directionally solidified powder compacts. The samples which were compacted and re-directionally solidified showed the highest transition temperature and widest transition range. This indicates that both steps, powder compaction and resolidification, determine the final superconducting properties of the material.

17. KEY WORDS

Superconductivity
Composites
Directional Solidification
Immiscible Materials

18. DISTRIBUTION STATEMENT

Unclassified - Unlimited

Subject Category 76

19. SECURITY CLASSIF. (of this report)	20. SECURITY CLASSIF. (of this page)	21. NO. OF PAGES	22. PRICE
Unclassified	Unclassified	41	A03

For sale by National Technical Information Service, Springfield, Virginia 22161
NASA-Langley, 1983

3 1 1U,H, 830310 S00903DS
DEPT OF THE AIR FORCE
AF WEAPONS LABORATORY
ATTN: TECHNICAL LIBRARY (SUL)
KIRTLAND AFB NM 87117